Mechanics of soft-solid–liquid-crystal interfaces

Alejandro D. Rey
Department of Chemical Engineering, McGill University, 3610 University Street, Montreal, Quebec, Canada H3A 2B2
(Received 13 October 2004; revised manuscript received 21 March 2005; published 22 July 2005)

The interfacial mechanics of soft elastic solids and nematic liquid crystals is presented. The theory can be applied to interfaces involving gels, elastomers, biomaterials, and thermotropic nematic liquid crystals. A model of anisotropic elastic interfaces is formulated and used to derive two fundamental capillary quantities: (i) interfacial torques on the nematic orientation, and (ii) capillary pressure. The couplings between soft-solid deformation and liquid-crystal anisotropic interfacial tension is shown to lead to strain-induced anchoring transitions, and strain-induced morphological instabilities.

DOI: 10.1103/PhysRevE.72.011706 PACS number(s): 61.30.Hn

I. INTRODUCTION

Liquid crystals are anisotropic viscoelastic materials used in the manufacture of elctrooptical systems, temperature and chemical sensors, structural composites, and carbon fibers [1–5]. In many of these applications, deformable liquid-crystal–soft-solid interfaces play a significant role. For example, the use of liquid-crystal vision to detect protein adsorption and biomolecular interaction involves interfaces between liquid crystals and deformable biological layers [5]. Assembly of phospholipids at the interface between liquid crystals and aqueous phases [5] is another example of an elastic anisotropic surface, where the adsorbed phosphipid layer is well known [6] to contribute to the surface elasticity and where the anisotropy comes through the liquid crystalline phase. In addition, liquid crystal ordering is found in many biological systems, where the substrate is likely to be a soft elastic solid [7]. Moreover, it has been found experimentally that confined liquid crystal between soft solids can deform the surface through the action of stresses in the confined liquid crystals [8]. These few examples and experimental evidence [8] highlight the need for a fundamental understanding of deformable soft-solid–liquid-crystal interfaces. The term soft solid in this paper refers to materials such as polymer gels, biological tissues and materials, and elastomers, with a typical modulus of elasticity of the order of 10^3 Pa.

Elastocapillary phenomena in soft-solid–isotropic-liquid interfaces is an active area of research, since fundamental processes such as elastic wetting and dewetting involve contributions from soft-solid strain [9]. For these isotropic interfaces, it is found that interface tension creates interface distortions in the vicinity of contact lines that are balanced by solid stress [10–14]. Deformable solid-solid interfaces have also received attention since stress is a driving force for interface structuring [15–18]. An example is the Grinfeld instability, in which the flat interface of a strained solid can relieve stress by interface buckling [16,18]. In anisotropic solids it has already been demonstrated that interface strain and interface orientation contribute to the interfacial energy [17,18]. The coupling between strain and interface orientation provides a pathway to structure interfaces by strain release [17]. Elastocapillarity in liquid-crystal–soft-solid interfaces provides a fertile ground to exploit interface structuring by coupling soft-solid elasticity with the anisotropic interface tension of liquid crystals.

In anisotropic interfaces of deformable solid films, the expression of the interface tension that captures observed morphological transitions is [18,19]

$$\gamma = \gamma_{\mathrm{iso}} + \gamma_{\mathrm{s}}(\mathbf{k},\mathbf{b}_{\mathrm{s}}), \tag{1}$$

where γ_{iso} is the isotropic and $\gamma_{\mathrm{s}}(\mathbf{k},\mathbf{b}_{\mathrm{s}})$ the strain contribution, $\mathbf{k}$ is the unit normal, and $\mathbf{b}_{\mathrm{s}}$ is the elastic deformation or strain in the current configuration. On the other hand, for nematic liquid-crystal surfaces and interfaces, a well-established interface energy is known as the Rapini-Papoular energy [20–22]:

$$\gamma(\mathbf{k},\mathbf{n}) = \gamma_{\mathrm{iso}} + \gamma_{\mathrm{an}}(\mathbf{k},\mathbf{n}), \tag{2}$$

where γ_{iso} is the isotropic and $\gamma_{\mathrm{an}}(\mathbf{k},\mathbf{n})$ the anisotropic contribution, and $\mathbf{n}$ is the interface average molecular orientation, or director. Based on these well-established interface tension expressions for liquid crystals and anisotropic solids, it follows that for interfaces between soft solids and nematic liquid crystals we can expect that the interface energy combines the soft-solid deformation and the anisotropic nature of nematics, and should be given by

$$\gamma(\mathbf{k},\mathbf{n},\mathbf{b}_{\mathrm{s}}) = \gamma_{\mathrm{iso}} + \gamma_{\mathrm{s}}(\mathbf{k},\mathbf{n},\mathbf{b}_{\mathrm{s}}) + \gamma_{\mathrm{an}}(\mathbf{k},\mathbf{n}). \tag{3}$$

Given this orientation-shape-strain dependent interface tension, the issue then becomes to determine the fundamental capillary quantities [19,23,24]: (i) interfacial torques that determine the nematic average molecular orientation $\mathbf{n}$, (ii) capillary pressures that determine the interface shape, and (iii) tangential Marangoni forces $\mathcal{I}$ along the interface.

Figure 1 shows a schematic, adapted from [25], of the four basic surface deformation modes: extension, shear, bending, and twisting. In this paper the energy associated with these surface deformations is taken into account. Figure 2 shows a schematic of a shear deformation for homeotropic anchoring (top), and a shear deformation for planar anchoring (bottom). In this paper the energies associated with surface deformation depend on the director surface orientation, and hence the energy associated with the upper right state (sheared homeotropic surface patch) is different than the one corresponding to the lower right state (sheared planar surface

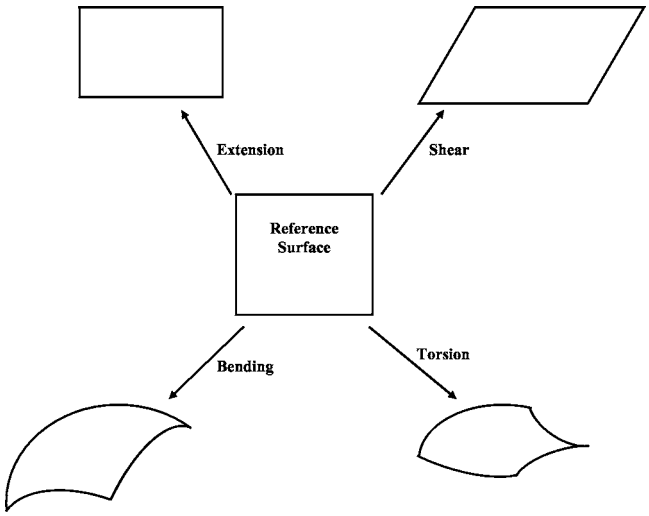

FIG. 1. Schematic of the four basic deformation modes of a square reference surface: extension, shear, bending, and twisting. Adapted from [25].

patch). This paper analyzes the additional contributions that arise when coupling surface deformation and director anchoring. It should be mentioned that the sheared homeotropic surface patch represents an isotropic surface, while the sheared planar surface patch has maximum anisotropy, since the director lies on the surface at a specific direction. This paper also elucidates the role of anisotropy on surface deformations.

The objectives of this paper are (1) to present an interfacial tension model based on well-established liquid-crystal interface physics and deformable solid film elasticity, (2) to use the theory to determine the two fundamental capillary quantities (interface orientation and interface shape), and (3) to provide examples of expected phenomena. Emphasis is placed on interface processes, but the derivations of the full set of bulk and interface balance equations is necessary to extract the expressions that describe the capillary processes.

The organization of this paper is as follows. Appendix A presents derivations of the geometry, and deformations of an anisotropic elastic interface, including the bulk and interface

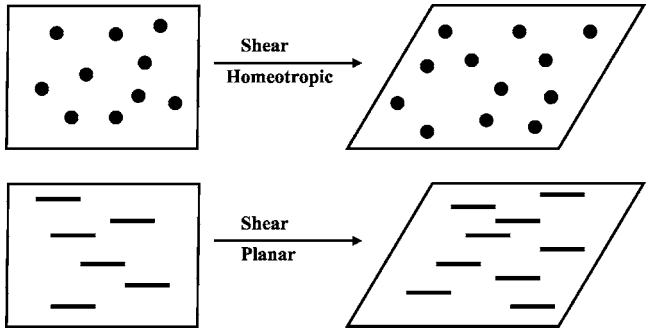

FIG. 2. Schematic of the shear deformation of the square reference surface patch, with homeotropic (top) and planar orientation (bottom). The dots (upper figures) indicate that the directors are normal to the surface, and the rods (bottom figures) indicate that the directors (average molecular orientation) are tangential to the surface patch.

Finger strain tensor, used throughout the paper. Section II presents the geometry of solid-liquid crystal system, and presents the force and torque balance equations, needed to describe interfacial processes. Details of the derivations of the balance equations are given in Appendix B while Appendix C presents the bulk elastic energies, the bulk stress tensors, and the bulk torques and couples. Section III presents the interfacial energy and discusses the coupling between deformation and orientation. Section IV presents the derivation of the interfacial stress tensor. Appendix D presents the specific contributions to the interface stress tensor arising from solid elasticity. Section V presents the Cahn-Hoffman capillary vector, used to compute capillary pressure. Section VI presents expressions used to analyze two capillary processes: (a) interface torque and interface orientation, and (b) capillary pressure and interface shape equation. Section VII presents the following applications for the two capillary processes: (a) the interface torque equation is used to show strain-induced interface orientation transitions, and (b) the capillary pressure equation is used to show strain-induced interface shape undulations.

II. INTERFACIAL GEOMETRY AND BALANCE EQUATIONS

In this section we present a complete set of force and torque balance equations for soft-solid–nematic-liquid-crystal interface phases. The detailed derivations are shown in Appendix B; since interfacial balance equations are derived in conjunction with bulk balance equations, the latter are also included in Appendix B. Since liquid crystals are anisotropic materials [22], the interactions across the interface includes not only forces but also couples [23]. In nematic liquid crystals, couple stresses arise due to director gradients, such that elastic torques are generated between neighboring domains attempting to eliminate the gradients (for an example, see p. 158 of [23]). An important issue is to find a suitable framework for interfaces between elastic isotropic solids and elastic anisotropic liquid crystals. In this paper we use the approach of the polar nematic model [26], which is equivalent the Leslie-Ericksen model and has proven useful to model contact line and capillary processes [26,27]. In the original Leslie-Ericksen model the director equation is given in terms of torques [22], while in the polar nematic version the director equation is given in terms of asymmetric stress vector and gradients of couple stresses [26]. The notion of couple stresses appears in most theories of materials with microstructure, and hence the use of the polar nematic model helps establish the connections between liquid crystal theories and polar fluid theories [26].

In this paper we analyze the statics of a soft-solid (SS)–nematic (N) liquid-crystal interface. The nematic bulk region is $\mathcal{R}^{\mathrm{N}}$ and the soft solid region is $\mathcal{R}^{\mathrm{SS}}$. The total bulk region $\mathcal{R}$ is the union of the two bulk regions: $\mathcal{R}=\mathcal{R}^{\mathrm{N}}+\mathcal{R}^{\mathrm{SS}}$. The outer bounding interfaces of the two bulk regions are, respectively, $\mathcal{S}^{\mathrm{N}},\mathcal{S}^{\mathrm{SS}}$. The outward bounding interface of $\mathcal{R}$ is $\mathcal{S}$ and is the union of the two interfaces: $\mathcal{S}=\mathcal{S}^{\mathrm{N}}+\mathcal{S}^{\mathrm{SS}}$. The interface of discontinuity between $\mathcal{R}^{\mathrm{N}}$ and $\mathcal{R}^{\mathrm{SS}}$ is Σ. The outer bounding edge of Σ is $\mathcal{C}$. The total bounding interface for the

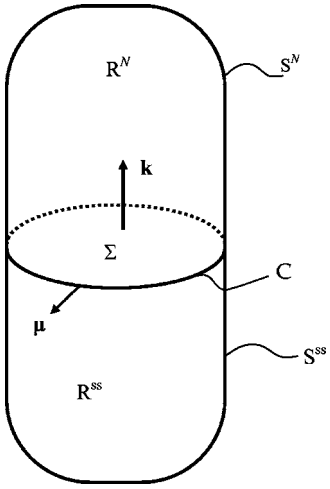

FIG. 3. Schematic of the geometry and definition of the volumes $(\mathcal{R}^{\mathrm{N}},\mathcal{R}^{\mathrm{SS}})$, bounding interfaces $(\mathcal{S}^{\mathrm{N}},\mathcal{S}^{\mathrm{SS}})$, interface of discontinuity (Σ), edge $(\mathcal{C})$, and normal vectors $(\boldsymbol{\xi},\boldsymbol{\mu})$.

nematic phase is $\Sigma+\mathcal{S}^{\mathrm{N}}$. The unit vector $\mathbf{k}$ is the normal to the interface of discontinuity Σ and is directed from $\mathcal{R}^{\mathrm{SS}}$ into $\mathcal{R}^{\mathrm{N}}$. The outward unit normal to edge $\mathcal{C}$ is $\boldsymbol{\mu}$. Figure 3 shows a schematic of the bulk and interfacial geometry and definition of the volumes $(\mathcal{R}^{\mathrm{N}},\mathcal{R}^{\mathrm{SS}})$, bounding interfaces $(\mathcal{S}^{\mathrm{N}},\mathcal{S}^{\mathrm{SS}})$, interface of discontinuity (Σ), edge $(\mathcal{C})$ of the interface of discontinuity Σ, and normal vectors $(\mathbf{k},\boldsymbol{\mu})$. The tensor notation used in this paper is

$$\begin{aligned}(\mathbf{A}\cdot\mathbf{n})_{\alpha} &= A_{\alpha\beta}n_{\beta};(\mathbf{A}\cdot\mathbf{B})_{\alpha\beta}\\ &= A_{\alpha\chi}B_{\chi\beta};(\nabla\cdot\mathbf{A})_{\alpha}\\ &= \nabla_{\beta}\mathbf{A}_{\beta\alpha};A_{\alpha\beta}\\ &= \partial f/\partial\nabla_{\alpha}n_{\beta}.\end{aligned}$$

To derive the bulk and interfacial force balance equations we need to introduce the following stress tensors: bulk stress tensors, $\mathbf{T}_{\mathrm{b}}^{\mathrm{i}}$ (energy/volume), interface stress tensor $\mathbf{T}_{\mathrm{s}}$ (energy/area); the superscript "i" in $\mathbf{T}_{\mathrm{b}}^{\mathrm{i}}$ refers to the phase: $i=N$ (nematic liquid crystal) and $i=\mathrm{SS}$ (soft solid). $\mathbf{T}_{\mathrm{b}}^{\mathrm{N}}$ is the stress tensor in the nematic phase and $\mathbf{T}_{\mathrm{b}}^{\mathrm{SS}}$ is the stress tensor in the soft solid phase. The dimensionality of the bulk and interface stress tensors are $\mathbf{T}_{\mathrm{b}}^{\mathrm{N}}$ and $\mathbf{T}_{\mathrm{b}}^{\mathrm{SS}}$ are 3×3, and $\mathbf{T}_{\mathrm{s}}$ is 2×3. The soft-solid phase is isotropic and hence the bulk stress tensor is symmetric: $T_{\mathrm{b}\alpha\beta}^{\mathrm{SS}}=T_{\mathrm{b}\beta\alpha}^{\mathrm{SS}}$. To derive the bulk and interfacial torque balance equations we need to introduce the following duals [23]: $\mathbf{T}_{\mathrm{bx}}^{\mathrm{N}}=-\boldsymbol{\varepsilon}:\mathbf{T}_{\mathrm{b}}^{\mathrm{N}}$ for the nematic bulk phase, and $\mathbf{T}_{\mathrm{sx}}=-\boldsymbol{\varepsilon}:\mathbf{T}_{\mathrm{s}}$ for the interface; following traditional usage, the second subscript "x" denotes dual and $\boldsymbol{\varepsilon}$ is the 3D alternator tensor. The dual vectors contain the asymmetric information of the stress tensors. In addition we have to take into account the nematic bulk couple stress tensor $\mathbf{C}_{\mathrm{b}}^{\mathrm{N}}$ (energy/area) [22,26,27]. In this paper we assume that the interface energy is independent of orientation gradients and hence no interface couples $(\mathbf{C}_{\mathrm{s}}=\mathbf{0})$ are taken into account; if warranted by experimental observation, interface couple effects can be incorporated in future work. Due to their 2×3 dimensionality the interface stress tensor $\mathbf{T}_{\mathrm{s}}$ obey [23]

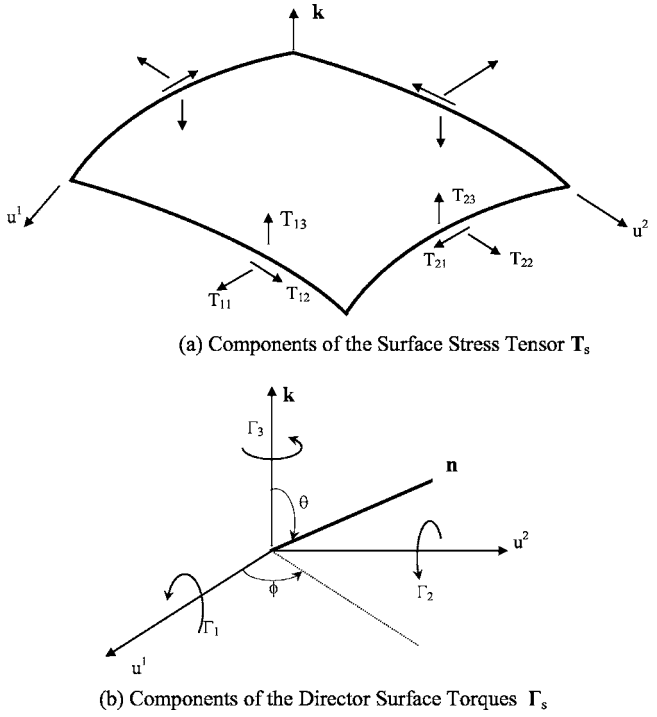

FIG. 4. (a) Schematic of the components of the interfacial stress tensor $\mathbf{T}_{\mathrm{s}}$, on a surface patch defined by a local coordinate system (u^1,u^2) and the unit normal $\mathbf{k}$. Surface stresses have tangential $(T_{11},T_{22},T_{21},T_{12})$ and bending (T_{13},T_{23}) components. (b) Schematic of the torques acting on the surface director on a surface patch defined by a surface coordinate system (u^1,u^2) and the outward unit normal $\mathbf{k}$. Here θ is the polar angle, and ϕ the azimuthal angle.

$$\mathbf{T}_{\mathrm{s}}=\mathbf{I}_{\mathrm{s}}\cdot\mathbf{T}_{\mathrm{s}}, \tag{4}$$

where $\mathbf{I}_{\mathrm{s}}=\mathbf{I}_{\mathrm{s}}^{\mathrm{T}}=\mathbf{I}-\mathbf{k}\cdot\mathbf{k}$ is the interface idem factor and $\mathbf{k}$ is the unit normal. Figure 4(a) shows a schematic of the components of the surface stresses $\mathbf{T}_{\mathrm{s}}$, on a surface patch defined by a local coordinate system (u^1,u^2) and the unit normal $\mathbf{k}$. Surface stresses have tangential $(T_{11},T_{22},T_{21},T_{12})$ and bending (T_{13},T_{23}) components and arise through the interactions between the soft solid and the nematic liquid crystal. Jumps in the bulk stresses $[\mathbf{k}\cdot\mathbf{T}_{\mathrm{b}}]$ and couple stresses across interfaces are defined by [24]

$$[\mathbf{k}\cdot\mathbf{T}_{\mathrm{b}}]=\mathbf{k}\cdot[\mathbf{T}_{\mathrm{b}}^{\mathrm{SS}}-\mathbf{T}_{\mathrm{b}}^{\mathrm{N}}], \tag{5a}$$

$$[\mathbf{k}\cdot\mathbf{C}_{\mathrm{b}}]=\mathbf{k}\cdot[\mathbf{C}_{\mathrm{b}}^{\mathrm{SS}}-\mathbf{C}_{\mathrm{b}}^{\mathrm{N}}]=\mathbf{k}\cdot\mathbf{C}_{\mathrm{b}}^{\mathrm{N}}, \tag{5b}$$

where $\mathbf{C}_{\mathrm{b}}^{\mathrm{SS}}=\mathbf{0}$ was used. The bulk $\boldsymbol{\Gamma}_{\mathrm{b}}$ and interface $\boldsymbol{\Gamma}_{\mathrm{s}}$ torques acting on the director are given in terms of the stress duals and couples as follows [23]:

$$\boldsymbol{\Gamma}_{\mathrm{b}}=\mathbf{T}_{\mathrm{bx}}+\nabla\cdot\mathbf{C}_{\mathrm{b}} \tag{6a}$$

$$\boldsymbol{\Gamma}_{\mathrm{s}}=\mathbf{T}_{\mathrm{sx}}+\nabla_{\mathrm{s}}\cdot\mathbf{C}_{\mathrm{s}}=\mathbf{T}_{\mathrm{sx}}, \tag{6b}$$

where $\mathbf{C}_{\mathrm{s}}=\mathbf{0}$ was used. The original Leslie-Ericksen model uses torques $(\boldsymbol{\Gamma}_{\mathrm{b}},\boldsymbol{\Gamma}_{\mathrm{s}})$, while the polar nematic version of the model uses stress duals $(\mathbf{T}_{\mathrm{bx}},\mathbf{T}_{\mathrm{sx}})$ and couples $(\mathbf{C}_{\mathrm{b}},\mathbf{C}_{\mathrm{s}})$. In the absence of interface couples $(\mathbf{C}_{\mathrm{s}}=\mathbf{0})$, the interface

torques $\mathbf{\Gamma}_s$ acting on the director arise from asymmetric stress ($\mathbf{T}_{sx}$). Figure 4(b) shows a schematic of the torques acting on the surface director on a surface patch defined by a surface coordinate system (u^1,u^2) and the outward unit normal $\mathbf{k}$. Under the action of (Γ_1,Γ_2) the director tilts away or toward the unit normal $\mathbf{k}$; here θ is the polar angle. On the other hand, (Γ_3) causes a precession around $\mathbf{k}$, described by change in the the azimuthal angle ϕ. In the present model $\Gamma_3=0$ and the surface imparts no preference on the selection of the azimuthal angle. When all the interfacial energy is independent of the azimuthal angles, the state is known as conical degeneracy (p. 110 of [22]).

The derivation of the bulk and interface force balance equation starts with a balance of all forces acting on the bounding surface S of R, the edge C of the interface, the bulk R, and interface Σ [24]:

$$\int_S (\boldsymbol{\nu}\cdot\mathbf{T}_b)dA+\int_C \boldsymbol{\mu}\cdot\mathbf{T}_s d+\int_R \rho_b\mathbf{z}_b dV+\int_\Sigma \rho_s\mathbf{z}_s dA=0, \tag{7}$$

where (ρ_b,ρ_s) are the bulk and interfacial densities, and $(\mathbf{z}_b,\mathbf{z}_s)$ are the bulk and interface body forces per unit mass. As shown in Appendix B, use of 3D and 2D divergence theorems in conjunction with Eq. (7) leads, after some algebra, to the following bulk and interface force balance equations:

$$\textit{bulk elastic solid } (R^{SS}):\quad \nabla\cdot\mathbf{T}_b^{SS}+\rho_b^{SS}\mathbf{z}_b=\mathbf{0}, \tag{8}$$

$$\textit{bulk nematic liquid crystal } (R^{N}):\quad \nabla\cdot\mathbf{T}_b^{N}+\rho_b^{N}\mathbf{z}_b=\mathbf{0}, \tag{9}$$

$$\textit{interface } (\Sigma):\quad \nabla_s\cdot\mathbf{T}_s+\rho_s\mathbf{z}_s+\mathbf{k}\cdot[\mathbf{T}_b{}^{SS}-\mathbf{T}_b{}^{N}]=\mathbf{0}. \tag{10}$$

Equation (11) is the force balance equation at an interface and states that the stress jump at the interface $[\mathbf{k}\cdot(\mathbf{T}_b{}^{SS}-\mathbf{T}_b{}^{N})]$ is balanced by gradients in surface stresses and body forces $(\nabla_s\cdot\mathbf{T}_s+\rho_s\mathbf{z}_s)$. Soft-solid elasticity effects are incorporated in $(\mathbf{T}_s,\mathbf{T}_b{}^{SS})$ and in the shape of the interface $(\mathbf{k})$. For rigid interfaces $\mathbf{k}$ is known and interface shape is not part of the problem, while for soft interfaces $\mathbf{k}$ is unknown and must be found using Eq. (10).

The derivation of the static bulk and interface torque moment balance equation starts with a balance of all moments acting on the system [27]:

$$\mathbf{L}_S+\mathbf{L}_C+\mathbf{L}_R+\mathbf{L}_\Sigma=\mathbf{0} \tag{11}$$

where $\mathbf{L}_S$ the moment acting on the bounding surface S, $\mathbf{L}_C$ on the edge C of the interface, $\mathbf{L}_R$ on the bulk R, and $\mathbf{L}_\Sigma$ on the interface Σ. The moment acting on the bounding surface $\mathbf{L}_S$ [27],

$$\mathbf{L}_S=\int_S \mathbf{r}\times(\boldsymbol{\nu}\cdot\mathbf{T}_b)dA+\int_S(\boldsymbol{\nu}\cdot\mathbf{C}_b)dA \tag{12}$$

is the sum of stress vector moment $\mathbf{r}\times(\boldsymbol{\nu}\cdot\mathbf{T}_b)$ and the bulk couple vector $\boldsymbol{\nu}\cdot\mathbf{C}_b$ contributions. For nematic liquid crystals the bulk couple tensor $\mathbf{C}_b$ is due to director orientation gradients:

$$\mathbf{C}_b=\frac{\partial f_g^N}{\partial\nabla\mathbf{n}}\cdot\boldsymbol{\varepsilon}\cdot\mathbf{n}=\mathbf{n}\times\frac{\partial f_g^N}{\partial\nabla_\mathbf{n}}, \tag{13}$$

where f_g^N is the Frank elastic energy [22], defined in Eq. (4); Eq. (13) is discussed in conjunction with Eq. (3.115) of [22] and Eq. (15) of [26(a)]. For isotropic materials $\mathbf{C}_b=\mathbf{0}$, and only the stress terms appears in Eq. (12). The moment acting on the edge $\mathbf{L}_C$ [27],

$$\mathbf{L}_C=\int_C(\mathbf{r}\times\boldsymbol{\mu}\cdot\mathbf{T}_s)d \tag{14}$$

arises from the interface stress vector moment $\mathbf{r}\times(\boldsymbol{\nu}\cdot\mathbf{T}_b)$; in the present model the surface couple vector $\boldsymbol{\nu}\cdot\mathbf{C}_S$ is assumed to be zero, which implies that there are no energy penalties due to interfacial director gradients: $\gamma\neq\gamma(\nabla_s\mathbf{n})$. The moment acting on the bulk $\mathbf{L}_R$ is given by [24]

$$\mathbf{L}_R=\int_R \mathbf{r}\times(\rho_b\mathbf{z}_b)dV \tag{15}$$

and arises from moments of the bulk body forces $\rho_b\mathbf{z}_b$. The moment acting on the interface $\mathbf{L}_\Sigma$ is given by [24]

$$\mathbf{L}_\Sigma=\int_R \mathbf{r}\times(\rho_s\mathbf{z}_s)dV \tag{16}$$

and arises from moments of the interface body forces $\rho_S\mathbf{z}_S$. As shown in Appendix B, use of the divergence theorem in conjunction with Eqs. (11) and (13)–(16) leads, after some algebra, to the following bulk and interfacial torque balance equations:

$$\textit{bulk nematic liquid crystal } (R^{N}):\quad \mathbf{T}_{bx}^{N}+\nabla\cdot\mathbf{C}_b^{N}=\mathbf{0}, \tag{17}$$

$$\textit{interface } (\Sigma):\quad \mathbf{T}_{sx}-\mathbf{k}\cdot\mathbf{C}_b^{N}=\mathbf{0}. \tag{18}$$

Equation (17) is the 3D torque balance equation of nematostatics [22,27]. Equation (18) is the corresponding 2D torque balance equation of interfacial nematostatics [27]. In Eq. (18) no couple from the soft solid is present because this material is isotropic: $\mathbf{C}_b^{SS}=\mathbf{0}$. If the contacting phases are assumed to be isotropic, the balance equation reduced to the statement that the interfacial stress is symmetric: $\mathbf{T}_{sx}=\mathbf{0}$, in agreement with fluid-fluid interfaces [24].

The interfacial balance equations will be used in Sec. VII to analyze interfacial orientation transitions and strain-induced shape transitions.

III. INTERFACE ELASTICITY

The physics of nematic surfaces and interfaces with rigid solids or fluids has been widely studied [see, for example, [20,21,27–37]], while here we study deformable elastic solid-nematic–liquid-crystal interfaces. The total interfacial elastic energy adopted in this work is given by

$$F_s = \int_s \gamma dA, \tag{19a}$$

$$\gamma = \gamma_{iso} + \gamma_{an} + \gamma_c, \tag{19b}$$

where s is the current interface, γ is the interfacial tension, γ_{iso} is the isotropic interfacial tension, γ_{an} is the anchoring interfacial tension [20,21,35], and γ_c is the strain-orientation coupling contribution due to the presence of a deformable elastic solid; if $\gamma_c=0$ we recover an expression widely used in the field [20,21,35]. The isotropic interfacial tension γ_{iso} is independent of the director orientation $\mathbf{n}$ and of the unit normal $\mathbf{k}$. The interfacial energy density γ_{an} is known as the anchoring energy, and it represents the anisotropic contribution to the interfacial free energy density associated with deviations of the director from its preferred orientation due to the action of torques driven by bulk distortions or external fields. The preferred orientation or easy axis can be (i) parallel to the interface unit normal $\mathbf{k}$, also known as homeotropic, (ii) tilted with respect to $\mathbf{k}$, or (iii) tangential to the interface, also known as planar orientation [20,21,35]. For the tilted and planar orientations, unique, multiple, or degenerate stability can arise depending on the nature of the material in contact with the nematic liquid crystal [35]. In the present paper we consider unique stability, with the preferred orientation being either homeotropic or degenerate planar, meaning that when the preferred orientation is tangential to the interface all tangential directions are energetically equivalent.

The anchoring γ_{an} energy is given by the Rapini-Papoular model [20,21,35]:

$$\gamma_{an} = \frac{\gamma_2}{2}(\mathbf{n}\cdot\mathbf{k})^2, \tag{20}$$

where γ_2 is the anchoring energy coefficients or anchoring strengths that represent the polar anchoring strength for changes in the angle between $\mathbf{n}$ and $\mathbf{k}$. The director orientation that minimizes γ_{an} depends on the sign of γ_2 [20,21,35]. All of the interfacial anisotropic effects are contained in γ_{an}. The anchoring-strain coupling energy γ_c is

$$\gamma_c = \gamma_b I^4_{\alpha\beta\chi\delta}(b_{s\alpha\beta}n_\chi n_\delta + n_\alpha n_\beta b_{s\chi\delta}) + \gamma_{bk}\Psi^4_{\alpha\beta\chi\delta} \times (b_{s\alpha\beta}n_\chi n_\delta + n_\alpha n_\beta b_{s\chi\delta}), \tag{21}$$

$$I^4_{\alpha\beta\chi\delta} = \frac{1}{2}(I_{s\alpha\chi}I_{s\beta\delta} + I_{s\alpha\delta}I_{s\beta\chi}),$$

$$\Psi^4_{\alpha\beta\chi\delta} = \frac{1}{4}(I_{s\alpha\beta}k_\chi k_\delta + I_{s\chi\delta}k_\alpha k_\beta), \tag{22}$$

$$\gamma_c = \underbrace{\gamma_b \mathbf{b}_s:\mathbf{nn}}_{\text{strain-induced orientation}} + \underbrace{\frac{\gamma_{bk}}{2}(\mathbf{I}_s:\mathbf{b}_s)(\mathbf{n}\cdot\mathbf{k})^2}_{\text{anchoring effect}}, \tag{23}$$

where the first term describes strain-induced orientation, and the second takes into account renormalization of the anchoring coefficient due to the presence of deformation. Similar expressions to Eq. (28) arise in elastic surface models of thin films [18]. The interfacial tension then becomes

$$\gamma - \gamma_{iso} = \gamma_{Tan} + \gamma_b \mathbf{b}_s:\mathbf{nn}, \tag{24a}$$

$$\gamma_{Tan} = \left[\frac{\gamma_2}{2} + \frac{\gamma_{bk}}{2}(\mathbf{I}_s:\mathbf{b}_s)\right](\mathbf{n}\cdot\mathbf{k})^2, \tag{24b}$$

where γ_{Tan} is the total anchoring energy. As shown below, different combinations of these different tensions $(\gamma, \gamma_{an}, \gamma_{Tan}, \gamma_c)$, arise when calculating torques, and capillary pressures.

IV. INTERFACIAL STRESS TENSOR

The expression of the elastic interface stress tensor $\mathbf{T}_s$ is found by noting that $\gamma=\gamma(\mathbf{I}_s,\mathbf{b}_s,\mathbf{n},\mathbf{k})$ and by using a variation of the interfacial tension with respect to the three displacement-related fields [26,33]. Taking into account the three arguments in the interfacial tension we find that the interface stress tensor $\mathbf{T}_s$ is

$$\mathbf{T}_s(\mathbf{I}_s,\mathbf{b}_s,\mathbf{n},\mathbf{k}) = \underbrace{\mathbf{T}^n_s}_{\text{normal}} + \underbrace{\mathbf{T}^{SS}_s}_{\text{elastic}} + \underbrace{\mathbf{T}^b_s}_{\text{bending}}, \tag{25}$$

where $\mathbf{T}^n_s$ is the normal (tension) 2×2 interfacial stress tensor exhibit by all interfaces, $\mathbf{T}^{SS}_s$ is the symmetric 2×2 elastic stress tensor, and $\mathbf{T}^b_s$ is the 1×2 bending interfacial stress tensor. The nature of the components of the 2×3 interfacial stress tensor $\mathbf{T}_s$ components is [23,38]

$$\mathbf{T}_s = \begin{bmatrix} T^{SS}_{11} + T^n_{11} & T^{SS}_{21} & T^b_{13} \\ T^{SS}_{12} & T^{SS}_{22} + T^n_{22} & T^b_{23} \end{bmatrix}. \tag{26}$$

Next we briefly describe the origin and nature of the three stresses: $\mathbf{T}^n_s$, $\mathbf{T}^{SS}_s$, and $\mathbf{T}^b_s$. The normal stress $\mathbf{T}^n_s$ is the 2D analogue of pressure in 3D and is given by the pure tangential diagonal tensor [23,24]:

$$\mathbf{T}^n_s = \gamma\mathbf{I}_s. \tag{27}$$

This stress appears in all isotropic and anisotropic interfaces [23], but in the present model, the normal stress components (T^n_{11}, T^n_{22}) are functions of $(\mathbf{I}_s,\mathbf{b}_s,\mathbf{n},\mathbf{k})$. Expanding the differential $d\gamma$ at constant $\mathbf{n}$ we find

$$d\gamma = \mathbf{T}^{SS}_s:d\mathbf{b}_s - (\mathbf{T}^b_s\cdot\mathbf{k})\cdot d\mathbf{k}, \tag{28}$$

where the conjugate to the interface Finger tensor $\mathbf{b}_s$ is the elastic stress tensor $\mathbf{T}^{SS}_s$, and the conjugate to the outward unit normal $\mathbf{k}$ is the bending stress vector $\mathbf{T}^b_s\cdot\mathbf{k}$, defined by

$$\mathbf{T}^b_s\cdot\mathbf{k} = -\mathbf{I}_s\cdot\left(\frac{\partial\gamma}{\partial\mathbf{k}}\right)_{\mathbf{n},\mathbf{b}_s} \tag{29a}$$

$$\rightarrow \mathbf{T}^{SS}_s = \left(\frac{\partial\gamma}{\partial\mathbf{b}_s}\right)^{[s]}_{\mathbf{n},\mathbf{k}}. \tag{29b}$$

Here the arrow means that Eq. (29a) implies Eq. (29b). The superscript $[s]$ denotes tangential and symmetric tensor and this restriction must be imposed because $\mathbf{b}_s$ is tangential and symmetric; in addition the projector tensor $\mathbf{I}_s$ appears in Eq. (29a) because the left-hand side (i.e., $\mathbf{T}^b_s\cdot\mathbf{k}$) is a tangential vector and hence it must obey $\mathbf{k}\cdot(\mathbf{T}^b_s\cdot\mathbf{k})=0$. The tangential

symmetric elastic stress tensor $\mathbf{T}_s^{SS}$ is obtained using Eq. (29a) and it is given by

$$\mathbf{T}_s^{SS} = (\mathbf{T}_s^{SS})^T = \left(\frac{\partial \gamma}{\partial \mathbf{b}_s}\right)_{\mathbf{n},\mathbf{k}}^{[s]} = \frac{1}{2}\left(\mathbf{I}_s \cdot \left(\frac{\partial \gamma}{\partial \mathbf{b}_s}\right)_{\mathbf{n},\mathbf{k}} \cdot \mathbf{I}_s + \mathbf{I}_s \cdot \left(\frac{\partial \gamma}{\partial \mathbf{b}_s}\right)_{\mathbf{n},\mathbf{k}}^{T} = \cdot \mathbf{I}_s\right). \tag{30}$$

The detailed expressions for the solid contributions to the interfacial stress tensor are given in Appendix C. The elastic stress tensor $\mathbf{T}_s^{SS}$ contains shear and normal stresses and obeys the following restrictions:

$$\mathbf{T}_s^{SS} \cdot \mathbf{k} = 0, \tag{31a}$$

$$\mathbf{T}_s^{SS} = \mathbf{I}_s \cdot \mathbf{T}_s^{SS} = \mathbf{T}_s^{SS} \cdot \mathbf{I}_s. \tag{31b}$$

The bending stress tensor $\mathbf{T}_s^b$ arises when the interfacial tension is anisotropic and varies with surface tilting. Using Eq. (29b) for the bending stress vector $\mathbf{T}_s^b \cdot \mathbf{k}$, it follows that the bending stress tensor $\mathbf{T}_s^b$ is

$$\mathbf{T}_s^b = -\mathbf{I}_s \cdot \left(\frac{\partial \gamma}{\partial \mathbf{k}}\right)_{\mathbf{n},\mathbf{b}_s} \mathbf{k}. \tag{32}$$

For isotropic interfaces bending stresses are always zero because the interfacial energy does not depend on the unit normal $\mathbf{k}$ [27]. For anisotropic interfaces bending stresses are zero when either of these conditions hold:

$$\mathbf{I}_s \cdot \partial \gamma / \partial \mathbf{k} = \mathbf{0}, \quad \text{or} \quad \partial \gamma / \partial \mathbf{k} = \mathbf{0}. \tag{33}$$

The bending stress tensor $\mathbf{T}_s^b$ obeys the following restrictions [23,27]:

$$\mathbf{T}_s^b = \mathbf{T}_s^b \cdot \mathbf{k}\mathbf{k}, \tag{34a}$$

$$\mathbf{T}_s^b = \mathbf{I}_s \cdot \mathbf{T}_s^{SS}. \tag{34b}$$

Given the symmetry of the three interfacial stress components, the dual of the interfacial stress tensor is

$$\mathbf{T}_{sx} = -\boldsymbol{\varepsilon} : \mathbf{T}_s = -\boldsymbol{\varepsilon} : \mathbf{T}_s^b = \mathbf{k} \times \mathbf{I}_s \cdot \left(\frac{\partial \gamma}{\partial \mathbf{k}}\right)_{\mathbf{n},\mathbf{b}_s} \tag{35}$$

and indicates that interfacial torques arise due to bending stresses. No torques are associated with diagonal normal stress $\mathbf{T}_s^n$ or symmetric elastic stresses $\mathbf{T}_s^{SS}$. Expressions (34a) and (35) were given before [27], and Eq. (34b) is the analogue of the bulk stress in elastic solids [see Eq. (B6)].

In summary, when comparing elastic and inelastic interfaces we find

$$\textit{elastic}: \ \mathbf{T}_s = \mathbf{T}_s^n + \mathbf{T}_s^{SS} + \mathbf{T}_s^b, \quad \textit{inelastic}: \ \mathbf{T}_s = \mathbf{T}_s^n + \mathbf{T}_s^b. \tag{36}$$

Since in general the surface divergence of the elastic stresses contribute both to tangential and normal forces [23]:

$$\nabla_s \cdot \mathbf{T}_s^s = (T_{s,\alpha}^{s\alpha\beta})\mathbf{a}_\beta + (\mathbf{m} : \mathbf{T}_s^s)\mathbf{k} \tag{37}$$

predictions from inelastic model would be incomplete; in Eq. (37) $T_{s,\alpha}^{s\alpha\beta}$ is the covariant derivative of the contravariant components of $\mathbf{T}_s$ [23], $\mathbf{m}$ is the curvature tensor [see Eq. (18)], and $\mathbf{a}_\beta$ is the surface basis vector [see Eq. (A1c)].

V. CAHN-HOFFMAN CAPILLARY VECTOR

Anisotropic interfaces differ from isotropic interfaces by the fact that the interfacial tension is a function of interface orientation. Hoffman and Cahn introduced the concept of capillary vector to describe the mechanics and thermodynamics of anisotropic crystal surfaces [19,39,40]. Based on the Cahn-Hoffman anisotropic crystal capillary vector model, the corresponding equations for liquid crystal interfaces were derived and used to analyze capillary instabilities and contact line problems [41,42]. In these previous works it was demonstrated that working with the capillary vector lead to a great simplification in the description and analysis of capillary processes, as well as a clear physical picture. Here we extend this useful approach and derive the Cahn-Hoffman capillary vector in the presence of elastic stresses.

For anisotropic liquid crystal interfaces, changes in interfacial energy can be driven by changes in interfacial area (expansion or contraction) and changes in interface inclination (tilting towards or away from the director). Describing the interface with spherical coordinates (r, θ, ϕ), using as surface coordinates $(u^1 = \theta, u^2 = \phi)$ and surface unit normal $\mathbf{k} = \boldsymbol{\delta}_r$, and assuming that $\gamma(\theta, \phi)$, the capillary vector $\boldsymbol{\xi}$ is defined by [19,39,40]

$$\boldsymbol{\xi} = \nabla(r\gamma) = \frac{\partial (r\gamma)}{\partial r}\mathbf{k} + \frac{1}{r}\frac{\partial (r\gamma)}{\partial \theta}\boldsymbol{\delta}_\theta + \frac{1}{r \sin\theta}\frac{\partial (r\gamma)}{\partial \phi}\boldsymbol{\delta}_\phi, \tag{38}$$

where $(\boldsymbol{\delta}_\theta, \boldsymbol{\delta}_\phi)$ are the orthogonal unit vectors in the (θ, ϕ) directions, respectively; for additional applications see discussion of Eq. (1.5) in [39]. Upon simplification Eq. (38) gives

$$\boldsymbol{\xi} = \gamma\mathbf{k} + (\mathbf{I} - \mathbf{k}\mathbf{k}) \cdot \frac{\partial \gamma}{\partial \mathbf{k}} \tag{39}$$

The projection tensor $(\mathbf{I} - \mathbf{k}\mathbf{k})$ appears in Eq. (39) because only the tangential part of the vector $\partial\gamma/\partial\mathbf{k}$ needs to be taken into account. The capillary vector $\boldsymbol{\xi}$ satisfies the relation $\boldsymbol{\xi} \cdot \mathbf{k} = \gamma$ [19,39,40]. The normal component of the capillary vector $\boldsymbol{\xi}_\perp = \gamma\mathbf{k}$ describes changes due to area size, and the tangential component $\boldsymbol{\xi}_\parallel = (\mathbf{I} - \mathbf{k}k) \cdot \partial\gamma/\partial\mathbf{k}$ describes changes due to area tilting. We note that the capillary vector $\boldsymbol{\chi}$ is a function of the director $\mathbf{n}$, the unit normal $\mathbf{k}$, and the interface Finger tensor $\mathbf{b}_s$. Direct comparison between Eqs. (27), (32), and (39) shows that the relations between $\boldsymbol{\xi}$ and normal and bending stresses are

$$\mathbf{T}_s^n = (\boldsymbol{\xi}_\perp \cdot \mathbf{k})\mathbf{I}_s = \gamma\mathbf{I}_s, \tag{40a}$$

$$\mathbf{T}_s^b = -\boldsymbol{\xi}_\parallel\mathbf{k} = -\mathbf{I}_s \cdot \frac{\partial \gamma}{\partial \mathbf{k}}\mathbf{k}. \tag{40b}$$

Using Eqs. (25), (27), (32), (40a), and (40b) the interfacial stress tensor $\mathbf{T}_s$ can be rewritten in a very compact form as

$$\mathbf{T}_s = \boldsymbol{\xi} \cdot \boldsymbol{\Psi} + \mathbf{T}_s^{SS}, \tag{41a}$$

$$\boldsymbol{\Psi} = \mathbf{k}\mathbf{I}_s - \mathbf{I}_s\mathbf{k}, \tag{41b}$$

where $\boldsymbol{\Psi}$ is a third order asymmetric geometry tensor that map the capillary vector into a interfacial stress. Using the definition of the geometry tensor $\boldsymbol{\Psi}$ [Eq. (41b)] in Eq. (41a) gives a compact expression for the interfacial stress tensor $\mathbf{T}_s$:

$$\mathbf{T}_s = (\boldsymbol{\xi}\cdot\mathbf{k})\mathbf{I}_s + \mathbf{T}_s^{SS} - (\boldsymbol{\xi}\cdot\mathbf{I}_s)\mathbf{k} \tag{42}$$

and shows that solid elasticity introduces extensional and shear stresses; the exact expression for $\mathbf{T}_s^{SS}$ is given in Eq. (D2).

In partial summary, this section derived the equation for the interface stress tensor $\mathbf{T}_s$, which is need to compute capillary pressure [23,24]. In the absence of solid elasticity, the capillary vector $\boldsymbol{\xi}$ and the interface stress given in Eqs. (39), (40a), and (40b) agree with previous results [41,42]. The main differences between elastic and inelastic surfaces are

$$\textit{elastic}: \quad \mathbf{T}_s = \boldsymbol{\xi}(\mathbf{n},\mathbf{k},\mathbf{b}_s)\cdot\boldsymbol{\Psi} + \mathbf{T}_s^{SS}, \tag{43a}$$

$$\textit{inelastic}: \quad \mathbf{T}_s = \boldsymbol{\xi}(\mathbf{n},\mathbf{k})\cdot\boldsymbol{\Psi} \tag{43b}$$

as a consequence shear stresses are not accounted for in the classical inelastic formulation. As mentioned above, the presence and importance of interfacial elastic stresses in instabilities and pattern formation are well known [18,19].

VI. CAPILLARY PROCESSES

In this section we use the theory to derive expressions for two fundamental capillary processes: (i) interface torques, and (ii) capillary pressure. The interface torques determine the director interface orientation, and the capillary pressure determines the interface shape [23,24].

A. Interface torques and interface orientation

Since we neglect interfacial torques ($\mathbf{C}_s=0$), the interface torques arise only from asymmetric stress [see Eq. (6b)]. To find the expression for the interface torque $\boldsymbol{\Gamma}_S$ we use an analogous procedure as for bulk torques [Eqs. (B12) and Ref. [22]]. Using the principle of rotational invariance [32], which states that the energy does not change upon a solid body rotation, we find, following the standard operations given in [22,26,32], that

$$\varepsilon_{\alpha\beta\chi}\left(\frac{\partial\gamma}{\partial n_\chi}n_\beta + \frac{\partial\gamma}{\partial k_\chi}k_\beta + \frac{\partial\gamma}{\partial b_{s\delta\beta}}b_{s\delta\beta} + \frac{\partial\gamma}{\partial b_{s\chi\delta}}b_{s\beta\delta}\right) = 0. \tag{44}$$

Thus the second order tensor contained in the parenthesis in Eq. (44) must be symmetric. Using the principle of rotational invariance [Eq. (44)] and some algebraic manipulations shown in Appendix F, we obtain the following expression for the interfacial torque vector:

$$\boldsymbol{\Gamma}_s = \mathbf{n}\times\mathbf{h}_{s\,\mathrm{Tan}} = -\mathbf{n}\times\frac{\partial\gamma_{\mathrm{Tan}}}{\partial\mathbf{n}}, \tag{45}$$

where $\mathbf{h}_{s\,\mathrm{Tan}}$ is the interface molecular field, and where the subscript "Tan" was added to highlight the fact that the interfacial torque is only a function of γ_{Tan}. It is worth emphasizing that Eqs. (45) shows that the torque on the director $\boldsymbol{\Gamma}_s$ only involves the total anchoring energy γ_{Tan} [see Eq. (29b)] and is the analogue to the well-known [22] bulk equation (B10). Using Eqs. (35) and (45) we find that the following equality holds:

$$-\mathbf{n}\times\frac{\partial\gamma_{\mathrm{Tan}}}{\partial\mathbf{n}} = \mathbf{k}\times\mathbf{I}_s\cdot\left(\frac{\partial\gamma}{\partial\mathbf{k}}\right)_{\mathbf{n},\mathbf{b}_s}. \tag{46}$$

Equation (46) establishes the consistency between stress dual $\mathbf{T}_{sx}$ and director torque $\boldsymbol{\Gamma}_s$ expressions, since according to Eq. (6b) they should be equal: $\boldsymbol{\Gamma}_s=\mathbf{T}_{sx}$. Equation (46) also establishes the fact that the torques acting on the director have no component along the unit normal: $\boldsymbol{\Gamma}_s\cdot\mathbf{k}=0$, and hence there is no surface-driven preferable angle on a circle centered on the unit normal, a fact known as conical degeneracy of the director around $\mathbf{k}$ [22].

In partial summary, in this section we use an efficient method to derive the director torques at the surface. The important difference between inelastic and elastic interfaces in this case is the anchoring energy involved in the torque expressions:

$$\textit{elastic}: \quad \boldsymbol{\Gamma}_s = -\mathbf{n}\times\frac{\partial\gamma_{\mathrm{Tan}}}{\partial\mathbf{n}}, \quad \textit{inelastic}: \quad \boldsymbol{\Gamma}_s = -\mathbf{n}\times\frac{\partial\gamma_{\mathrm{an}}}{\partial\mathbf{n}} \tag{47}$$

and hence using the inelastic expression will be incomplete.

B. Capillary pressures and interface shape equation

The interface shape equation [23] is given by the normal component of the interface force balance equation (10):

$$-\rho_s\mathbf{z}_s\cdot\mathbf{k} - \mathbf{k}\cdot[\mathbf{T}_b{}^{S} - \mathbf{T}_b{}^{N}]\cdot\mathbf{k} = -p_c = (\nabla_s\cdot\mathbf{T}_s)\cdot\mathbf{k}, \tag{48}$$

where p_c is the capillary pressure. This equation is also known as the interface shape equation. As a consequence of the dependence of the interface tension on deformation, orientation, and interface tilting, the capillary pressure for the soft-solid-nematic interface is given by the sum of Laplacian ($-p_c^{\mathrm{Laplacian}}$) and non-Laplacian ($-p_c^{\mathrm{non\text{-}Laplacian}}$) contributions. To find the capillary pressure associated with elastic stresses we use the divergence expression (37) for tangential tensors and find upon use of Eq. (D2)

$$\begin{aligned}(\nabla_s\cdot\mathbf{T}_s^{SS})\cdot\mathbf{k} &= \mathbf{T}_s^{SS}:\mathbf{m}\\ &= -p_c^{\mathrm{stress}}\\ &= \mathbf{T}_s^{SS}:\mathbf{m}\\ &= [(\gamma_{bk}-\gamma_b)(\mathbf{n}\cdot\mathbf{k})^2]H + \gamma_b(\mathbf{n}_\parallel\mathbf{n}_\parallel:\mathbf{m}).\end{aligned} \tag{49}$$

The capillary pressure associated with elastic stresses vanishes for homeotropic orientation ($\mathbf{n}=\mathbf{k}$).

To find all of the contributions to the capillary pressure we use Eq. (41a) for $\mathbf{T}_s$ and find that $-p_c$ is given by the divergence of the capillary vector and a solid stress term:

$$-p_c = -\nabla_s \cdot \boldsymbol{\xi} + \mathbf{T}_s^{SS}:\mathbf{m}$$
$$= \underset{\text{area size}}{\frac{\partial \boldsymbol{\xi}_\perp}{\partial \mathbf{k}}:\mathbf{m}} + \underset{\text{area tilting}}{\frac{\partial \boldsymbol{\xi}_\parallel}{\partial \mathbf{k}}:\mathbf{m}} - \underset{\text{director curvature}}{\frac{\partial \boldsymbol{\xi}_\parallel}{\partial \mathbf{n}}:(\nabla_s \mathbf{n})^T} - \underset{\text{area deformation}}{\frac{\partial \boldsymbol{\xi}_\parallel}{\partial \mathbf{b}_s}(\nabla_s \mathbf{b}_s)^T}$$
$$+ \underset{\text{stress}}{\mathbf{T}_s^{SS}:\mathbf{m}}, \tag{50}$$

where the first term on the right-hand side is the Laplacian pressure term due to changes in area size found in all materials [23], the second term is due to energy changes due to area tilting, the third is due to energy changes due to director curvature, the fourth is due to energy changes by area deformation, and the last is due to elastic stress; the symbol ( ) denotes a triple contraction. The full expressions for $-p_c$, found by using the capillary vector [Eq. (39)], and the specific expressions of all terms are presented in Appendix E. Equation (50) clearly demonstrates that the classical Laplace pressure is just one of five contributions, and that pressure drops may be sustained in the absence of curvature ($\mathbf{m}=0$) by four distinct mechanisms.

In partial summary, an efficient derivation of the capillary pressure was presented using the capillary vector $\boldsymbol{\xi}$, and the physical meaning of five different capillary pressures was identified. The main difference between the capillary pressure of elastic and inelastic surfaces is

$$\textit{elastic}: \quad -p_c = -\nabla_s \cdot \boldsymbol{\xi}(\mathbf{n},\mathbf{k},\mathbf{b}_s) + \mathbf{T}_s^{SS}:\mathbf{m}, \tag{51a}$$

$$\textit{inelastic}: \quad -p_c = -\nabla_s \cdot \boldsymbol{\xi}(\mathbf{n},\mathbf{k}). \tag{51b}$$

It can then be concluded that the inelastic expression has no shear contributions and an incomplete capillary vector.

VII. APPLICATIONS

In this section we use the theory to calculate the effect of strain on the two fundamental capillary processes: (a) interface orientation, and (b) interface shape, as follows.

(a) In the first example the interface shape is fixed and the director reorients due to elastic torques generated by an external load acting on the solid. This case arises when the energy costs due to interface area increases $|\nabla_s \cdot \boldsymbol{\xi}_\parallel|$ are greater than the energy savings due to interface tilting $|\nabla_s \cdot \boldsymbol{\xi}_\perp|$

$$|\nabla_s \cdot \boldsymbol{\xi}_\parallel| \gg |\nabla_s \cdot \boldsymbol{\xi}_\perp|. \tag{52}$$

In this case shape undulations that increase interface area are not possible, but strain-induced director tilting on a flat surface is possible if

$$\left|\frac{\partial \gamma_c}{\partial \mathbf{n}}\right| > \left|\frac{\partial \gamma_{an}}{\partial \mathbf{n}}\right|. \tag{53}$$

This equation states that it is easier to tilt the director on a flat surface than undulate the surface with constant and fixed anchoring.

(b) In the second application the energy costs due to interface area increases are less than the energy savings due to interface tilting:

$$|\nabla_s \cdot \boldsymbol{\xi}_\parallel| \ll |\nabla_s \cdot \boldsymbol{\xi}_\perp|. \tag{54}$$

In this case undulations that increase interface area are possible, if the strain effect on interface tilting overcomes the resistance from a fixed director:

$$\left|\frac{\partial \gamma}{\partial \mathbf{k}}\right| > \left|\frac{\partial \gamma}{\partial \mathbf{n}}\right|. \tag{55}$$

A. Strain-driven anchoring transition

In this application we consider a flat and strained interface between a soft solid and a thick nematic film. The nematic film is sufficiently thick so that the bulk nematic elasticity plays no role. The key issue is to determine how strain affects director interface orientation. We use (x,y,z) frame and assume the director deviation from the unit normal is defined by $\mathbf{n}\cdot\mathbf{k}=\cos\theta$, $\mathbf{n}=(n_x,n_y,n_z)=(\sin\theta\cos\varphi,\sin\theta\sin\varphi,\cos\theta)$, where θ is the polar angle, and φ is the twist angle. We assume that a flat interface is subjected to a equibiaxial extension. For this case the unit tensors [found using Eqs. (A2), (A7), and (A12)], the interface deformation tensor $\mathbf{F}_s$, and interfacial Finger tensor $\mathbf{b}_s$ are given by

$$\mathbf{I}_s = \mathbf{I}_S = \mathbf{I} - \mathbf{k}\cdot\mathbf{k} = \mathbf{I} - \mathbf{K}\cdot\mathbf{K}, \quad \mathbf{F}_s = \begin{bmatrix} \lambda & 0 \\ 0 & \lambda \end{bmatrix},$$
$$\mathbf{b}_s = \begin{bmatrix} \lambda_2 & 0 \\ 0 & \lambda_2 \end{bmatrix}, \tag{56}$$

where λ is the stretch ratio. Since $|\nabla_s\cdot\boldsymbol{\xi}_\parallel| \gg |\nabla_s\cdot\boldsymbol{\xi}_\perp|$ [see Eq. (52)] holds, $\mathbf{k}=\mathbf{K}$ and no shape change is assumed to occur. The governing torque balance equations (18) for the tilt and twist angle become

$$\frac{\partial \gamma_{Tan}}{\partial \theta} = 0, \quad \frac{\partial \gamma_{Tan}}{\partial \varphi} = 0. \tag{57}$$

Using Eq. (24b) we find that the equilibrium twist angle obeys

$$[(-\gamma_{bk})(2\lambda^2) - \gamma_2]\sin\theta\cos\theta = 0, \tag{58}$$

and the twist angle is undetermined: $0 \leqslant \varphi \leqslant \pi$. The stable polar angle θ depends on the sign of the deformation-dependent coefficient in the brackets. The conditions leading to stable homeotropic ($\theta=0$) and planar ($\theta=\pi/2$) polar angles are

$$\theta = 0, \quad (-\gamma_{bk})(2\lambda^2) - \gamma_2 > 0,$$
$$\theta = \pi/2, (-\gamma_{bk})(2\lambda^2) - \gamma_2 < 0. \tag{59}$$

The critical stretching for a homeotropic-planar transition is

$$\lambda_c = \sqrt{\frac{\gamma_2}{2(-\gamma_{bk})}}. \tag{60}$$

Four different scenarios arise:

(i) $\gamma_2 < 0$ and $(-\gamma_{bk}) < 0$: The orientation is homeotropic if $\lambda < \lambda_c$, and and planar if $\lambda > \lambda_c$.

(ii) $\gamma_2 < 0$ and $(-\gamma_{bk}) > 0$: The orientation is always homeotropic.

(iii) $\gamma_2>0$ and $(-\gamma_{bk})>0$: The orientation is planar if $\lambda<\lambda_c$, and homeotropic if $\lambda>\lambda_c$.

(iii) $\gamma_2>0$ and $(-\gamma_{bk})<0$: The orientation is always planar.

This model predicts that biaxial extension strain-induced sign changes in the effective anchoring constant leads to anchoring transitions in the polar angle, while the azimuthal angle is degenerate. The effect of interface shear is beyond the scope of this paper, but it can be stated that certain parametric conditions lead to a planar anchoring with preferred twist angle.

B. Strain-driven shape distortion

In this section we explore the possibility of interface shape distortion of an initially flat interface through the action of an imposed planar extensional solid deformation. A similar instability but driven from elastic stress in the bulk of a liquid crystal in contact with a soft solid was recently reported [8]. The unit normal to the initial flat interface is, in a rectangular (x,y,z) coordinate system, $\mathbf{K}=\boldsymbol{\delta}_z$, where $\boldsymbol{\delta}_z$ is the unit vector in the z direction. We further assume that the director is initially homeotropic ($\mathbf{n}=\mathbf{K}$), which corresponds to $\lambda_2<0$. We wish to determine whether an interface undulation under a constant director field ($\mathbf{n}=\mathbf{K}$) can decrease the energy. Using Appendix A, the geometry and deformation of the flat interface are

$$\mathbf{n}=\mathbf{K}=\boldsymbol{\delta}_z, \tag{61a}$$

$$\mathbf{F}_b=\lambda_x\boldsymbol{\delta}_x\boldsymbol{\delta}_x+\boldsymbol{\delta}_y\boldsymbol{\delta}_y+\lambda_z\boldsymbol{\delta}_x\boldsymbol{\delta}_x, \tag{61b}$$

$$\mathbf{B}_b=\lambda_x^2\boldsymbol{\delta}_x\boldsymbol{\delta}_x+\boldsymbol{\delta}_y\boldsymbol{\delta}_y+\lambda_z^2\boldsymbol{\delta}_x\boldsymbol{\delta}_x, \tag{61c}$$

$$\mathbf{F}_S=\lambda_x\boldsymbol{\delta}_x\boldsymbol{\delta}_x+\boldsymbol{\delta}_y\boldsymbol{\delta}_y, \tag{62a}$$

$$\mathbf{B}_S=\lambda_x^2\boldsymbol{\delta}_x\boldsymbol{\delta}_x+\boldsymbol{\delta}_y\boldsymbol{\delta}_y. \tag{62b}$$

We subject the initially flat interface S to a small perturbation $\zeta(x)$ in the normal (z) direction:

$$\zeta(x)=\zeta_o\cos(\lambda x). \tag{63}$$

The unit normal $\mathbf{k}$ and unit tangent $\mathbf{e}$ to the distorted interface s are given by

$$\mathbf{k}=\mathbf{K}-\partial_x\zeta\boldsymbol{\delta}_x=\mathbf{K}+\zeta_o\sin(\lambda x)\boldsymbol{\delta}_x, \tag{64a}$$

$$\mathbf{e}=\boldsymbol{\delta}_x-\zeta_o\lambda\ \sin(\lambda x)\mathbf{K}, \tag{64b}$$

where (ζ_o,λ) are the amplitude and wave vector. Using Eqs. (61a)–(61c), (62a), (62b), (63), (64a), (64b), and (A14b)), it is found that the interface finger tensor $\mathbf{b}_s$ for the distorted interface is $\mathbf{b}_s=\mathbf{B}_s+\mathbf{o}(\zeta^2)$, where $\mathbf{o}(\zeta^2)$ indicates a perturbation tensor that is second order in the amplitude ζ_o. To determine the energy changes due to interface undulations, it is best to compute the capillary pressure, using Eq. (45). For weak deviations from homeotropic anchoring, the capillary pressure simplifies to

$$-p_c=-\nabla_s\cdot\boldsymbol{\xi}+\mathbf{T}_s^{SS}:\mathbf{m}=\Phi+\Delta(\zeta), \tag{65}$$

where Φ is a constant and $\Delta(\zeta)$ contains all the perturbation dependent terms. A perturbation $\zeta(x)$ decreases the interface energy when

$$\Delta(\zeta)>0. \tag{66}$$

According to Eq. (65), the capillary pressure for a homeotropic interface with a 1D periodic distortion is

$$-p_c=(\gamma-(\gamma_2+\gamma_{bk}\lambda^2))\kappa_1, \tag{67a}$$

$$\kappa_1=\partial_{xx}\zeta=-k^2\zeta, \tag{67b}$$

where κ_1 is the principal curvature due to the perturbation. Substituting Eqs. (67a) and (67b) into inequality (66) we find that the interface instability equation is given by

$$\Delta=-(\gamma-(\gamma_2+\gamma_{bk}\lambda^2))k^2>0. \tag{68}$$

Equation (68) shows that strain-induced undulation is possible if the energy increase due to undulation is overcome by the energy decrease due to tilting:

$$\underset{\text{energy increase for surface creation}}{\gamma} < \underset{\text{energy decrease by tilting}}{(\gamma_2+\gamma_{bk}\lambda^2)} \rightarrow 2\gamma_{iso}$$
$$-\gamma_2<\gamma_{bk}\lambda^2, \tag{69}$$

Since $2\gamma_{iso}$-$\gamma_2>0$ for all known systems, we reach the conclusion that stretching leads to interface undulation whenever

$$\gamma_{bk}>0,\lambda>\sqrt{\frac{2\gamma_{iso}-\gamma_2}{\gamma_{bk}}}. \tag{70}$$

The mechanism of strain-induced shape deformation is based on the fact that the solid deformation renormalizes the anchoring energy, such that increases in energy due to increases in interface area are overcome by decreases in energy due to interface tilting. In other words, even if undulations always increase surface area, tilting a sufficiently strained anisotropic surface may lead to a net energy decrease. A similar instability is discussed for anisotropic solid films on p. 617 of [18].

VIII. CONCLUSIONS

A mechanical theory for soft-solid–nematic-liquid-crystal interfaces has been formulated in terms of interfacial force and torque balance equations. The theory can be applied to interfaces involving gels, elastomers, biomaterials and thermotropic nematic liquid crystals. Inspired by elastic film physics [18], a constitutive interface energy equation that couples interface strain, director and interface orientation is formulated. The capillary pressure of soft-solid–liquid-crystal interfaces contains geometric and orientation curvature, as well as strain gradients effects, implying that pressure differentials exist even in flat interfaces. The interface torque equation shows that strain generates torques able to reorient the director. Applications of the theory to strain-

induced reorientation show that interface extensional deformations can tilt the director from its preferred orientation. Applications of the theory to strain-induced interface structuring shows that interface extensional deformations can periodically tilt the interface away from a flat configuration. This work shows that interface strain in soft solids is a possible mechanism for shape and structure generation in complex-fluids–soft-solid interfaces.

ACKNOWLEDGMENT

This work is supported by a grant from the Donors of The Petroleum Research Fund (PRF) administered by the American Chemical Society.

APPENDIX A

Geometry and deformation

The purpose of the appendix is to derive and discuss the bulk and interface Finger tensors used to describe defromations in elastic bulk and surface phases, and to present the geometry related quantities used throughout the paper.

In this paper we consider arbitrary deformations [43,44], beyond the linear regime. This may be necessary when considering arbitrary large bulk deformation processes that may couple to surface processes. Consider the distortion of a reference interface S into an interface s [43,44]. The material interface coordinates in the reference configuration are U^α, $\alpha=1,2$ and the material interface coordinates in the present configuration are u^α, $\alpha=1,2$. The configurations of the interface s and S are $\mathbf{x}_s=\mathbf{x}_s(u^\alpha)$, $\mathbf{X}_s=\mathbf{X}_s(U^\alpha)$, and the deformation is given by $u^\alpha=\phi^\alpha(\mathbf{U})$. The interface s can then be represented by $\mathbf{x}_s=\mathbf{x}_s(\phi^\alpha(\mathbf{U}))=\Xi_s^\alpha(\mathbf{U})$. The interface base vectors $\mathbf{a}_\alpha$, $\mathbf{A}_\alpha$, for s and S are

$$d\mathbf{x}_s=\frac{\partial \mathbf{x}_s}{\partial U^\alpha}dU^\alpha=\mathbf{a}_\alpha dU^\alpha, \tag{A1a}$$

$$d\mathbf{X}_s=\frac{\partial \mathbf{X}_s}{\partial U^\alpha}dU^\alpha=\mathbf{A}_\alpha dU^\alpha, \tag{A1b}$$

$$\mathbf{a}_\alpha=\frac{\partial \mathbf{x}_s}{\partial U^\alpha}, \tag{A1c}$$

$$\mathbf{A}_\alpha=\frac{\partial \mathbf{X}_s}{\partial U^\alpha} \tag{A1d}$$

and the corresponding interface matrix tensors $(a_{\alpha\beta},A_{\alpha\beta})$, determinants (a,A), and unit normals $(\mathbf{k},\mathbf{K})$ are

$$a_{\alpha\beta}=\mathbf{a}_\alpha\cdot\mathbf{a}_\beta, \tag{A2a}$$

$$A_{\alpha\beta}=\mathbf{A}_\alpha\cdot\mathbf{A}_\beta, \tag{A2b}$$

$$a=\det(a_{\alpha\beta})=|\mathbf{a}_1\times\mathbf{a}_2|^2, \tag{A2c}$$

$$A=\det(A_{\alpha\beta})=|\mathbf{A}_1\times\mathbf{A}_2|^2, \tag{A2d}$$

$$\mathbf{k}=\mathbf{a}_1\times\mathbf{a}_2/\sqrt{a}, \tag{A2e}$$

$$\mathbf{K}=\mathbf{A}_1\times\mathbf{A}_2/\sqrt{A}. \tag{A2f}$$

Reciprocal base vectors for s and S are

$$dU^\alpha=\frac{\partial U^\alpha}{\partial \mathbf{x}}\cdot d\mathbf{x}=\mathbf{a}^\alpha\cdot d\mathbf{x}, \tag{A3a}$$

$$dU^\alpha=\frac{\partial U^\alpha}{\partial \mathbf{X}}d\mathbf{X}=\mathbf{A}^\alpha d\mathbf{X}, \tag{A3b}$$

$$\mathbf{a}^\alpha=\frac{\partial U^\alpha}{\partial \mathbf{x}}, \tag{A3c}$$

$$\mathbf{A}^\alpha=\frac{\partial U^\alpha}{\partial \mathbf{X}}. \tag{A3d}$$

The interface unit tensor δ_α^β and interface idemfactor of s and S are defined by

$$\delta_\alpha^\beta=\mathbf{a}_\alpha\cdot\mathbf{a}^\beta, \tag{A4a}$$

$$\mathbf{I}_s=\mathbf{I}-\mathbf{kk}=\mathbf{I}_s^{\mathrm{T}}=\mathbf{a}_\alpha\mathbf{a}^\alpha=a_{\alpha\beta}\mathbf{a}^\alpha\mathbf{a}^\beta=a^{\alpha\beta}\mathbf{a}_\alpha\mathbf{a}_\beta, \tag{A4b}$$

$$\delta_\alpha^\beta=\mathbf{A}_\alpha\cdot\mathbf{A}^\beta, \tag{A5a}$$

$$\mathbf{I}_S=\mathbf{I}-\mathbf{KK}=\mathbf{I}_S^{\mathrm{T}}=\mathbf{A}_\alpha\mathbf{A}^\alpha=A_{\alpha\beta}\mathbf{A}^\alpha\mathbf{A}^\beta=\mathrm{A}^{\alpha\beta}\mathbf{A}_\alpha\mathbf{A}_\beta. \tag{A5b}$$

The interface curvature tensors $\mathbf{m}$ and $\mathbf{M}$ for s and S are

$$\mathbf{m}=-\nabla_s\mathbf{k}, \tag{A6a}$$

$$\nabla_s=\mathbf{I}_s\cdot\nabla=\frac{\partial}{\partial U^\alpha}\mathbf{a}^\alpha, \tag{A6b}$$

$$\mathbf{M}=-\nabla_S\mathbf{K}, \tag{A6c}$$

$$\nabla_S=\mathbf{I}_S\cdot\nabla=\frac{\partial}{\partial U^\alpha}\mathbf{A}^\alpha. \tag{A6d}$$

The interface deformation gradient F_s and its inverse F_s^{-1} are defined by

$$d\mathbf{x}_s=\mathbf{F}_s\cdot d\mathbf{X}_s, \tag{A7a}$$

$$\mathbf{F}_s=\frac{\partial \mathbf{x}_s}{\partial \mathbf{X}_s}=\frac{\partial \mathbf{x}_s}{\partial U^\alpha}\frac{\partial U^\alpha}{\partial \mathbf{X}_s}=\mathbf{a}_\alpha\mathbf{A}^\alpha, \tag{A7b}$$

$$d\mathbf{X}_s=\mathbf{F}_s^{-1}\cdot d\mathbf{x}_s, \tag{A8a}$$

$$\mathbf{F}_s^{-1}=\frac{\partial \mathbf{X}_s}{\partial \mathbf{x}_s}=\frac{\partial \mathbf{X}_s}{\partial U^\alpha}\frac{\partial U^\alpha}{\partial \mathbf{x}_s}=\mathbf{A}_\alpha\mathbf{a}^\alpha. \tag{A8b}$$

The deformation gradient tensors F transforms tangential vectors lying in S into vectors in s, in particular

$$\mathbf{a}_\alpha = \mathbf{F}_s \cdot \mathbf{A}^\alpha. \tag{A9}$$

The inverse deformation gradient tensors F^{-1} transforms tangential vectors lying in s into vectors in S, in particular

$$\mathbf{A}_\alpha = \mathbf{F}_s^{-1} \cdot \mathbf{a}^\alpha. \tag{A10}$$

It follows that the unit idem factors $\mathbf{I}_s$, $\mathbf{I}_S$ are given by

$$\mathbf{F}_s \cdot \mathbf{F}_s^{-1} = \mathbf{a}_\alpha \mathbf{a}^\alpha = \mathbf{I}_s = \mathbf{I} - \mathbf{kk}, \tag{A11a}$$

$$\mathbf{F}_s^{-1} \cdot \mathbf{F}_s = \mathbf{A}_\alpha \mathbf{A}^\alpha = \mathbf{I}_S = \mathbf{I} - \mathbf{KK}. \tag{A11b}$$

Using the deformation and inverse deformation we can define the symmetric positive definite interface Finger tensor $\mathbf{b}_s$:

$$\begin{aligned}\mathbf{b}_s &= \mathbf{F}_s \cdot \mathbf{F}_s^{\mathrm{T}} \\ &= \frac{\partial \mathbf{x}_s}{\partial \mathbf{X}_s} \cdot \left(\frac{\partial \mathbf{x}_s}{\partial \mathbf{X}_s} \right)^{\mathrm{T}} \\ &= \frac{\partial \mathbf{x}_s}{\partial U^\alpha} \frac{\partial U^\alpha}{\partial \mathbf{X}_s} \cdot \frac{\partial U^\beta}{\partial \mathbf{X}_s} \frac{\partial \mathbf{x}_s}{\partial U^\beta} \\ &= \mathbf{a}_\alpha \mathbf{a}_\beta (\mathbf{A}^\alpha \cdot \mathbf{A}^\beta) = \mathbf{a}_\alpha \mathbf{a}_\beta A^{\alpha\beta}.\end{aligned} \tag{A12}$$

The bulk Finger tensor $\mathbf{b}_b$ is given in terms of the bulk deformation gradient $\mathbf{F}_b$ and initial and final bulk position vectors $(\mathbf{X}_b, \mathbf{x}_b)$ as follows:

$$\mathbf{b}_b = \mathbf{F}_b \cdot \mathbf{F}_b^{\mathrm{T}} = \frac{\partial \mathbf{x}_b}{\partial \mathbf{X}_b} \cdot \left(\frac{\partial \mathbf{x}_b}{\partial \mathbf{X}_b} \right)^{\mathrm{T}}. \tag{A13}$$

In the case of bulk-surface affine deformation, the interface Finger tensor $\mathbf{b}_s$ in terms of $\mathbf{b}_b$ and unit normal $\mathbf{k}$ is

$$\mathbf{b}_s = (\mathbf{I}_s \cdot \mathbf{F} \cdot \mathbf{I}_S) \cdot (\mathbf{I}_S \cdot \mathbf{F}^{\mathrm{T}} \cdot \mathbf{I}_s) = \mathbf{I}_s \cdot (\mathbf{F} \cdot \mathbf{F}^{\mathrm{T}}) \cdot \mathbf{I}_s = \mathbf{I}_s \cdot \mathbf{b}_b \cdot \mathbf{I}_s. \tag{A14a}$$

$$\mathbf{b}_s(\mathbf{b}, \mathbf{k}) = \mathbf{b} - \mathbf{kk} \cdot \mathbf{b} - \mathbf{b} \cdot \mathbf{kk} + \mathbf{kk} \cdot \mathbf{b} \cdot \mathbf{kk}. \tag{A14b}$$

In the present configuration the mean curvature H and the interface curvature tensor $\mathbf{m}$ of the interface "s" are given by

$$H = -\frac{1}{2} \nabla_s \cdot \mathbf{k} = \frac{1}{2} \mathbf{I}_s : \mathbf{m} = -\frac{1}{2} \mathbf{I}_s : \nabla_s \mathbf{k} = \frac{1}{2} (\kappa_1 + \kappa_2), \tag{A15}$$

$$\mathbf{m} = -\nabla_s \mathbf{k} = \kappa_1 \mathbf{e}_1 \mathbf{e}_1 + \kappa_2 \mathbf{e}_2 \mathbf{e}_2, \tag{A16}$$

where $\{\kappa_i\}$ and $\{\mathbf{e}_i\}$, $i = 1, 2$, are the eigenvalues and eigenvectors of $\mathbf{m}$. The interface divergence of $\mathbf{I}_s$ is a normal vector: $\nabla_s \cdot \mathbf{I}_s = 2H\mathbf{k}$.

APPENDIX B

The purpose of this appendix is to present the derivation of the bulk force balance equations (8) and (9), the interface force balance equation (10), the bulk torque balance equation (17), and the interface torque balance equation (18).

1. Force balance equations

The force balance on the total volume of the system $\mathcal{R}$ is given by [24]

$$\int_S (\boldsymbol{\nu} \cdot \mathbf{T}_b) dA + \int_C \boldsymbol{\mu} \cdot \mathbf{T}_s d + \int_R \rho_b \mathbf{z}_b dV + \int_\Sigma \rho_s \mathbf{z}_s dA = 0. \tag{B1}$$

Using the divergence theorem in the presence of an interface of discontinuity the interface integral becomes [24]

$$\int_S \boldsymbol{\nu} \cdot \mathbf{T}_b dA = \int_R \nabla \cdot \mathbf{T}_b dV + \int_\Sigma [\mathbf{k} \cdot \mathbf{T}_b] dA. \tag{B2}$$

Using the interface divergence theorem the interface stress term becomes

$$\int_C \boldsymbol{\mu} \cdot \mathbf{T}_s d = \int_\Sigma \nabla_s \cdot \mathbf{T}_s dA. \tag{B3}$$

Collecting the bulk and interface contributions yields the following integral force balances:

$$\int_R (\nabla \cdot \mathbf{T}_b + \rho_b \mathbf{z}_b) dV = 0, \tag{B4a}$$

$$\int_\Sigma (\nabla_s \cdot \mathbf{T}_s + \rho_s \mathbf{z}_s + [\mathbf{k} \cdot \mathbf{T}_b]) dA = \mathbf{0}, \tag{B4b}$$

which are satisfied when

$$\nabla \cdot \mathbf{T}_b^{SS} + \rho_b^{SS} \mathbf{z}_b = \mathbf{0}, \tag{B5a}$$

$$\nabla \cdot \mathbf{T}_b^{N} + \rho_b^{N} \mathbf{z}_b = \mathbf{0}, \tag{B5b}$$

$$\nabla_s \cdot \mathbf{T}_s + \rho_s \mathbf{z}_s + \mathbf{k} \cdot [\mathbf{T}_b^{SS} - \mathbf{T}_b^{N}] = \mathbf{0}. \tag{B6}$$

2. Torque balance equations

The total torque balance equation resulting from forces and couples is [26]

$$\begin{aligned}&\int_S \mathbf{r} \times (\boldsymbol{\nu} \cdot \mathbf{T}_b) dA \\ &\quad + \int_C (\mathbf{r} \boldsymbol{\mu} \cdot \mathbf{T}_s) d + \int_S (\boldsymbol{\nu} \cdot \mathbf{C}_b) dA + \int_R \mathbf{r} \times (\rho_b \mathbf{z}_b) dV \\ &\quad + \int_\Sigma \mathbf{r} \times (\rho_s \mathbf{z}_s) dA = \mathbf{0}.\end{aligned} \tag{B7}$$

Next we use the bulk, and interface divergence theorem to evaluate the terms in Eq. (B7). Using this theorem on the bulk stress term yields

$$\int_S \mathbf{r} \times (\nu \cdot \mathbf{T}_b) dA = \int_R \nabla \cdot (\mathbf{r} \times \mathbf{T}_b) dV + \int_\Sigma \mathbf{r} \times [\mathbf{k} \cdot \mathbf{T}_b] dA. \tag{B8}$$

Using the following identity

$$\begin{aligned}\nabla \cdot (\mathbf{r} \times \mathbf{T}_b) &= \mathbf{r} \times (\nabla \cdot \mathbf{T}_b) + \mathbf{T}_{bx} \\ &= -\mathbf{r} \times (\rho_b \mathbf{z}_b) + \mathbf{T}_{bx}.\end{aligned} \tag{B9}$$

Substituting Eq. (B9) into Eq. (B8) gives

$$\int_S \mathbf{r}\times(\nu\cdot\mathbf{T}_b)dA=\int_R(-\mathbf{r}\times(\rho_b\mathbf{z}_b)+\mathbf{T}_{bx})dV+\int_\Sigma \mathbf{r}[\mathbf{k}\cdot\mathbf{T}_b]dA=\mathbf{0}. \tag{B10}$$

Similarly using the identity

$$\nabla\cdot(\mathbf{r}\times\mathbf{T}_s)=\mathbf{r}\times(\nabla\cdot\mathbf{T}_s)+\mathbf{T}_{sx}=-\mathbf{r}\times[\mathbf{k}\cdot\mathbf{T}_b]-\mathbf{r}\times\rho_s\mathbf{s}_s+\mathbf{T}_{sx} \tag{B11}$$

and upon a subsequent application of the interface divergence theorem gives

$$\int_C \mathbf{r}\times\boldsymbol{\mu}\cdot\mathbf{T}_s d=\int_\Sigma(-\mathbf{r}\times[\mathbf{k}\cdot\mathbf{T}_b]-\mathbf{r}\times\rho_s\mathbf{z}_s+\mathbf{T}_{sx})dA. \tag{B12}$$

We now proceed with the bulk couples and obtain

$$\int_S \nu\cdot\mathbf{C}_b dA=\int_R \nabla\cdot\mathbf{C}_b dV+\int_\Sigma[\mathbf{k}\cdot\mathbf{C}_b]dA. \tag{B13}$$

Collecting terms we find the bulk, interface, and line balances for the nematic phase:

$$\int_{R^N}\{\mathbf{T}_{bx}+\nabla\cdot\mathbf{C}_b\}dV=\mathbf{0},\quad \int_{R^{SS}}\{\mathbf{T}_{bx}+\nabla\cdot\mathbf{C}_b\}dV=\mathbf{0},\quad \int_\Sigma\{\mathbf{T}_{sx}+[\mathbf{k}\cdot\mathbf{C}_b]\}dA=\mathbf{0}. \tag{B14}$$

For an isotropic nonpolar soft solid $\mathbf{T}_{bx}^{SS}=\mathbf{0}$, $\mathbf{C}_b^{SS}=\mathbf{0}$. Thus the differential torque balances on the bulk nematic and the interface are

$$\mathbf{T}_x^N+\nabla\cdot\mathbf{C}_b^N=\mathbf{0}, \tag{B15a}$$

$$\mathbf{T}_{sx}-\mathbf{k}\cdot\mathbf{C}_b^N=\mathbf{0}. \tag{B15b}$$

In terms of torque vectors the balance equations (B15a) and (B15b) read

$$\boldsymbol{\Gamma}_b^N=\mathbf{0}, \tag{B16a}$$

$$\boldsymbol{\Gamma}_s-\mathbf{k}\cdot\mathbf{C}_b^N=\mathbf{0}. \tag{B16b}$$

The last equation indicates that the interface torques are balanced by the bulk couples.

APPENDIX C

The purpose of this appendix is to present the bulk energies, and then derive the bulk stress tensors, bulk couples, and the bulk torques. The bulk stress tensors appear in the force balance equations [Eqs. (8) and (9)]. The bulk couples and bulk torques appear in Eq. (17).

1. Bulk elasticity

In this section we present and discuss the elastic energies that arise when contacting a soft elastic solid with a nematic liquid crystal. The soft elastic solid occupies region R^{SS}, the nematic liquid crystal occupies region R^N, and the interfacial area is A. The total free energy of the system is [5,16,22]

$$F=F_b^{SS}=F_b^N+F_s, \tag{C1}$$

where F_b^{SS} is the total bulk solid free energy, F_b^N the total bulk nematic free energy, and F_s is the total interface free energy. For isotropic solids the energy is [27]

$$F_b^{SS}=\int\rho_b^{SS}\hat{f}_b^{SS}dV, \tag{C2a}$$

$$\hat{f}_b^{SS}=(\hat{K}_b/2-2\hat{G}_b/3)(\mathbf{b}_b:I)^2+\hat{G}_b\mathbf{b}_b:\mathbf{b}_b, \tag{C2b}$$

where the symbol $\hat{}$ denotes per unit mass. In Eq. (C2b), $\hat{K}_b$ is the bulk modulus of compressibility and $\hat{G}_b$ is the modulus of elasticity.

The total bulk nematic free energy F_b^N is given by [5,16,22]

$$F_b^N=\int f^N dV, \tag{C3a}$$

$$f^N=f_{iso}^N++f_g^N, \tag{C3b}$$

where f^N is the bulk energy per unit volume, f_{iso}^N the isotropic contribution per unit volume, and f_g^N is the gradient energy per unit volume known as Frank elastic energy. The energy per unit volume f_{iso}^N is independent of the director orientation and play no direct role in this paper. The Frank elastic energy per unit volume is given by [5,16,22]

$$f_g^N=\frac{1}{2}K_{11}(\nabla\cdot\mathbf{n})^2+\frac{1}{2}K_{22}(\mathbf{n}\cdot\nabla\times\mathbf{n})^2+\frac{1}{2}K_{33}|\mathbf{n}\times\nabla\times\mathbf{n}|^2, \tag{C4}$$

where $\{K_{ii}\}$; $ii=11,22,33$ are the splay, twist, bend (Frank) elastic constants.

2. Bulk stresses

At constant temperature the differential of the free energy per unit mass $\hat{f}_b^{SS}=f_b^{SS}/\rho^{SS}=\hat{f}_b^{SS}(\mathbf{b}_b)$ in the soft solid due to changes in density and deformation is

$$d\hat{f}_b^{SS}=\frac{t_{b\alpha\beta}^{dSS}}{\rho_b^{SS}}db_{b\alpha\beta}, \tag{C5}$$

where $t_{b\alpha\beta}^{dSS}$ is the elastic stress tensor. The symmetric bulk elastic stress due to distortion in the soft solid is according to classical elasticity:

$$\mathbf{T}_{\mathrm{b}}^{\mathrm{SSd}}(\mathbf{b}_{\mathrm{b}}) = (\mathbf{T}_{\mathrm{b}}^{\mathrm{SSd}})^{\mathrm{T}} = \rho_{\mathrm{b}}^{\mathrm{SS}}\left(\frac{\partial \hat{f}^{\mathrm{SS}}}{\partial \mathbf{b}_{\mathrm{s}}}\right) = 2G_{\mathrm{b}}\mathbf{b}_{\mathrm{b}} + (K_{\mathrm{b}} - 2G_{\mathrm{b}}/3)(\mathbf{I}:\mathbf{b}_{\mathrm{b}})\mathbf{I}, \tag{C6}$$

where $G_{\mathrm{b}}=\rho_{\mathrm{b}}^{\mathrm{SS}}\hat{G}_{\mathrm{b}}$, $K_{\mathrm{b}}=\rho_{\mathrm{b}}^{\mathrm{SS}}\hat{K}_{\mathrm{b}}$. Assuming an incompressible nematic phase, it can be shown that the asymmetric bulk stress in the nematic phase due to orientational gradients is

$$\mathbf{T}_{\mathrm{b}}^{\mathrm{N}}(\mathbf{n}, \nabla\mathbf{n}) = -p^{\mathrm{N}}\mathbf{I} + \mathbf{T}_{\mathrm{b}}^{\mathrm{Nd}}, \tag{C7a}$$

$$p^{\mathrm{N}} = (\mathbb{C} - f_{\mathrm{grav}}^{\mathrm{N}} - f_{\mathrm{g}}^{\mathrm{N}}), \tag{C7b}$$

$$\mathbf{T}_{\mathrm{b}\alpha\beta}^{\mathrm{Nd}} = -\frac{\partial f_{\mathrm{g}}^{\mathrm{N}}}{\partial \nabla_{\alpha} n_{\chi}}\nabla_{\beta} n_{\chi}, \tag{C7c}$$

where the gravitational energy $f_{\mathrm{grav}}^{\mathrm{N}}$ is defined by $\nabla f_{\mathrm{grav}}^{\mathrm{N}} = \rho_{\mathrm{b}}^{\mathrm{N}}\mathbf{z}_{\mathrm{b}}$ and where $\mathbb{C}$ is a constant.

3. Bulk couples and bulk torques

Bulk couples $\mathbf{C}_{\mathrm{b}}$ arise in the presence of orientation gradients ($\nabla\mathbf{n} \neq 0$). The derivation of the couple tensor is found in [22,26] and its expression is

$$C_{\mathrm{b}\delta\alpha} = \varepsilon_{\alpha\beta\chi} n_{\beta}\pi_{\mathrm{b}\delta\chi}; \quad \pi_{\mathrm{b}\delta\chi} = \frac{\partial f_{\mathrm{b}}^{\mathrm{N}}}{\partial \nabla_{\delta} n_{\chi}}. \tag{C8}$$

To find the relation between bulk couples $\mathbf{C}_{\mathrm{b}}$ and bulk torques $\mathbf{\Gamma}_{\mathrm{b}}$ it is best to use invariance relations under energy-preserving rotations. Using rotational invariance [32], it is found

$$\varepsilon_{\alpha\beta\chi}\left(\frac{\partial f_{\mathrm{b}}^{\mathrm{N}}}{\partial n_{\chi}} n_{\beta} + \frac{\partial f_{\mathrm{b}}^{\mathrm{N}}}{\partial \nabla_{\delta} n_{\chi}}\nabla_{\delta} n_{\beta} + \frac{\partial f_{\mathrm{b}}^{\mathrm{N}}}{\partial \nabla_{\chi} n_{\delta}}\nabla_{\beta} n_{\delta}\right) = \varepsilon_{\alpha\beta\chi}\left(\frac{\partial f_{\mathrm{b}}^{\mathrm{N}}}{\partial n_{\chi}} n_{\beta} - t_{\mathrm{b}\chi\beta}^{\mathrm{Nd}} + \pi_{\mathrm{b}\chi\delta}\nabla_{\beta} n_{\delta}\right) = 0, \tag{C9}$$

where the definition (C7c) for $t_{\mathrm{b}\chi\beta}^{\mathrm{Nd}}$ was used. Introducing the bulk molecular field $\mathbf{h}_{\mathrm{b}}$ [22],

$$h_{\mathrm{b}\alpha} = -\frac{\partial f_{\mathrm{b}}^{\mathrm{N}}}{\partial n_{\alpha}} + \nabla_{\delta}\left(\frac{\partial f_{\mathrm{b}}^{\mathrm{N}}}{\partial \nabla_{\delta} n_{\alpha}}\right) = -\frac{\partial f_{\mathrm{b}}^{\mathrm{N}}}{\partial n_{\alpha}} + \nabla_{\delta}\pi_{\mathrm{b}\delta\alpha}, \tag{C10}$$

Eq. (C9) gives

$$\varepsilon_{\alpha\beta\chi} t_{\mathrm{b}\beta\chi}^{\mathrm{Nd}} = \varepsilon_{\alpha\beta\chi} n_{\beta} h_{\mathrm{b}\chi} - \varepsilon_{\alpha\beta\chi} n_{\beta}\nabla_{\delta}\pi_{\mathrm{b}\delta\chi} - \varepsilon_{\alpha\beta\chi}\nabla_{\delta} n_{\beta}\pi_{\mathrm{b}\delta\chi} = \varepsilon_{\alpha\beta\chi} n_{\beta} h_{\mathrm{b}\chi} - \nabla_{\delta} C_{\mathrm{b}\delta\alpha}. \tag{C11}$$

Using Eq. (6a) we find that the torque is

$$\Gamma_{\mathrm{b}\alpha} = \varepsilon_{\alpha\beta\chi} T_{\mathrm{b}\beta\chi}^{\mathrm{Nd}} + \nabla_{\delta} C_{\mathrm{b}\delta\alpha} = \varepsilon_{\alpha\beta\chi} n_{\beta} h_{\mathrm{b}\chi}. \tag{C12}$$

Equation (C12) shows that bulk torques ($\mathbf{\Gamma}_{\mathrm{b}}$) arise due to asymmetric distortion stress ($\mathbf{T}_{\mathrm{b}}^{\mathrm{Nd}}$) and spatial gradients in the bulk couples stresses ($\nabla\cdot\mathbf{C}_{\mathrm{b}}$).

APPENDIX D

The purpose of this appendix is to present the expressions for the elastic solid contributions to the interfacial stress tensor, defined in Eq. (25). The specific contributions of solid deformation to the normal ($\mathbf{T}_{\mathrm{s}}^{\mathrm{Sn}}$), elastic ($\mathbf{T}_{\mathrm{s}}^{\mathrm{SS}}$), and bending ($\mathbf{T}_{\mathrm{s}}^{\mathrm{Sb}}$) stress components are found by replacing γ by γ_{c} in Eqs. (27), (30), and (32), and their expressions are

$$\mathbf{T}_{\mathrm{s}}^{\mathrm{Sn}} = (\gamma_{\mathrm{c}})\mathbf{I}_{\mathrm{s}} = \{\gamma_{\mathrm{b}}\mathbf{b}_{\mathrm{s}}:\mathbf{nn} + \gamma_{\mathrm{bk}}/2(\mathbf{I}_{\mathrm{s}}:\mathbf{b}_{\mathrm{s}})(\mathbf{n}\cdot\mathbf{k})^2\}\mathbf{I}_{\mathrm{s}}, \tag{D1}$$

$$\mathbf{T}_{\mathrm{s}}^{\mathrm{SS}} = \left(\frac{\partial(\gamma_{\mathrm{c}})}{\partial \mathbf{b}_{\mathrm{s}}}\right)_{\mathbf{k},\mathrm{n}}^{[\mathrm{S}]} = \frac{1}{2}[(\gamma_{\mathrm{bk}} - \gamma_{\mathrm{b}})(\mathbf{n}\cdot\mathbf{k})^2]\mathbf{I}_{\mathrm{s}} + \gamma_{\mathrm{b}}\mathbf{n}_{\parallel}\mathbf{n}_{\parallel}, \tag{D2}$$

$$\mathbf{T}_{\mathrm{s}}^{\mathrm{Sb}} = -\mathbf{I}_{\mathrm{s}}\cdot\left(\frac{\partial\gamma_{\mathrm{c}}}{\partial\mathbf{k}}\right)_{\mathbf{n},\mathbf{b}_{\mathrm{s}}}\mathbf{k} = -\gamma_{\mathrm{bk}}(\mathbf{I}_{\mathrm{s}}:\mathbf{b}_{\mathrm{s}})(\mathbf{n}\cdot\mathbf{k})(\mathbf{I}_{\mathrm{s}}\cdot\mathbf{n})\mathbf{k}, \tag{D3}$$

where $\mathbf{n}_{\parallel}=\mathbf{n}\cdot\mathbf{I}_{\mathrm{s}}$. Thus the solid deformation contributes to the three stress components: normal stress, shear stress, and bending stress. For homeotropic anchoring ($\mathbf{n}=\mathbf{k}$) the interface must behave as an isotropic material and the total solid stresses, as expected, reduces to an interface pressure:

$$\mathbf{T}_{\mathrm{s}}^{\mathrm{Sn}} + \mathbf{T}_{\mathrm{s}}^{\mathrm{SS}} + \mathbf{T}_{\mathrm{s}}^{\mathrm{Sb}} = \frac{\gamma_{\mathrm{bk}}}{2}(1 + (\mathbf{I}_{\mathrm{s}}:\mathbf{b}_{\mathrm{s}}))\mathbf{I}_{\mathrm{s}}. \tag{D4}$$

It is worth emphasizing that interfacial shear stress appears only in the presence of surface anisotropy, as expected.

APPENDIX E

The purpose of this appendix is to give the derivation of the interfacial torque equation (6b). The starting point of the derivation is Eq. (44). Expressing $(\partial\gamma/\partial k_{\chi})k_{\beta}$ in terms of the bending stress tensor [see Eq. (32)] we find

$$\frac{\partial\gamma}{\partial\mathbf{k}}\mathbf{k} = -\mathbf{T}_{\mathrm{s}}^{\mathrm{b}} + \mathbf{kk}\cdot\frac{\partial\gamma}{\partial\mathbf{k}}\mathbf{k}. \tag{E1}$$

Substituting Eq. (E1) in Eq. (44) and rearranging gives the dual of the interfacial bending stress tensor:

$$-\boldsymbol{\varepsilon}:\mathbf{T}_{\mathrm{s}}^{\mathrm{b}} = -\boldsymbol{\varepsilon}:\left(\frac{\partial\gamma}{\partial\mathbf{n}}\mathbf{n} + \mathbf{kk}\left(\mathbf{k}\cdot\frac{\partial\gamma}{\partial\mathbf{k}}\right) + \left(\frac{\partial\gamma}{\partial\mathbf{b}_{\mathrm{s}}}\right)^{\mathrm{T}}\cdot\mathbf{b}_{\mathrm{s}} + \frac{\partial\gamma}{\partial\mathbf{b}_{\mathrm{s}}}\cdot(\mathbf{b}_{\mathrm{s}})^{\mathrm{T}}\right). \tag{E2}$$

Using the relation between interfacial torques, the dual of the interfacial stress tensor and the dual of the bending stress tensor ($\mathbf{T}_{\mathrm{sx}}=-\boldsymbol{\varepsilon}:\mathbf{T}_{\mathrm{s}}=-\boldsymbol{\varepsilon}:\mathbf{T}_{\mathrm{s}}^{\mathrm{b}}$), demonstrated in Eq. (35), we find using Eqs. (6b) and (E2):

$$\mathbf{\Gamma}_{\mathrm{s}} = \mathbf{T}_{\mathrm{sx}} = -\boldsymbol{\varepsilon}:\mathbf{T}_{\mathrm{s}}^{\mathrm{b}} = -\boldsymbol{\varepsilon}:\left(\frac{\partial\gamma}{\partial\mathbf{n}}\mathbf{n} + \mathbf{kk}\left(\mathbf{k}\cdot\frac{\partial\gamma}{\partial\mathbf{k}}\right) + \left(\frac{\partial\gamma}{\partial\mathbf{b}_{\mathrm{s}}}\right)^{\mathrm{T}}\cdot\mathbf{b}_{\mathrm{s}} + \frac{\partial\gamma}{\partial\mathbf{b}_{\mathrm{s}}}\cdot(\mathbf{b}_{\mathrm{s}})^{\mathrm{T}}\right). \tag{E3}$$

Performing the tensor operations indicated in the right-hand side of Eq. (E3) gives after cancellation:

$$\Gamma_{s\alpha} = -\varepsilon_{\alpha\beta\chi} n_\beta \frac{\partial \gamma}{\partial n_\chi} - \varepsilon_{\alpha\beta\chi}\left(b_{s\delta\beta}\frac{\partial \gamma}{\partial b_{s\delta\chi}} + b_{s\alpha\beta}\frac{\partial \gamma}{\partial b_{s\chi\delta}}\right) = -\varepsilon_{\alpha\beta\chi} n_\beta \frac{\partial \gamma_{\mathrm{Tan}}}{\partial n_\chi}. \tag{E4}$$

Defining the interfacial molecular field $\mathbf{h}_{s\,\mathrm{Tan}}$ by

$$h_{s\mathrm{Tan},\chi} = -\frac{\partial \gamma_{\mathrm{Tan}}}{\partial n_\chi}, \tag{E5}$$

where the subscript was added to highlight the fact that it is a function of γ_{Tan}, finally gives the interfacial torque equation (45). It is worth emphasizing that Eq. (E4) shows that the torque on the director $\mathbf{\Gamma}_s$ only involves the total anchoring energy γ_{Tan} [see Eq. (24b)]. Eq. (E4) for $\mathbf{\Gamma}_s$ is the analogue to the bulk torque equation (C12).

APPENDIX F

The purpose of this appendix is to derive the full expressions of all the contributions appearing in the capillary pressure Eq. (50). The full expressions, found by using the capillary vector components [Eqs. (38) and (39)] and the expression of the solid stress tensor [Eq. (D2)] in Eq. (50), are as follows.

(a) Laplacian contribution:

$$-p_c^{\mathrm{Laplacian}} = -p_c^{\text{area size}} = \frac{\partial \boldsymbol{\xi}_\perp}{\partial \mathbf{k}} : \mathbf{m} = 2H\gamma = \gamma(\kappa_1 + \kappa_2). \tag{F1}$$

(b) Non-Laplacian contributions:

$$-p_c^{\text{area tilting}} = \frac{\partial \boldsymbol{\xi}_\parallel}{\partial \mathbf{k}} : \mathbf{m} = (\gamma_2 + \gamma_{\mathrm{bk}}(\mathbf{I}_s : \mathbf{b}_s))(\mathbf{nn} - (\mathbf{n}\cdot\mathbf{k})^2\mathbf{I}) : \mathbf{m} = (\gamma_2 + \gamma_{\mathrm{bk}}(\mathbf{I}_s : \mathbf{b}_s))\{[(\mathbf{n}\cdot\mathbf{e}_1)^2 - (\mathbf{n}\cdot\mathbf{k})^2]\kappa_1 + [(\mathbf{n}\cdot\mathbf{e}_2)^2 - (\mathbf{n}\cdot\mathbf{k})^2]\kappa_2\}, \tag{F2}$$

$$-p_c^{\text{director curvature}} = -\frac{\partial \boldsymbol{\xi}_\parallel}{\partial \mathbf{n}} : (\nabla_s \mathbf{n})^{\mathrm{T}} = -(\gamma_2 + \gamma_{\mathrm{bk}}(\mathbf{I}_s : \mathbf{b}_s)) \times \{\mathrm{tr}(\mathbf{kn}\nabla_s \mathbf{n}) + \mathrm{tr}(\mathbf{kn})\mathrm{tr}(\nabla_s \mathbf{n})\}, \tag{F3}$$

$$-p_c^{\text{strain}} = -\frac{\partial \boldsymbol{\xi}}{\partial \mathbf{b}_s}(\nabla_s \mathbf{b}_s)^{\mathrm{T}} = -\gamma_{\mathrm{bk}}(\mathbf{n}\cdot\mathbf{k})\{\mathrm{tr}(\mathbf{n}(\nabla_s \cdot \mathbf{b}_s)) - \mathrm{tr}(\mathbf{nk})\mathrm{tr}(\mathbf{k}(\nabla_s \cdot \mathbf{b}_s))\}, \tag{F4}$$

$$-p_c^{\text{stress}} = \mathbf{T}_s^{\mathrm{SS}} : \mathbf{m} = [(\gamma_{\mathrm{bk}} - \gamma_b)(\mathbf{n}\cdot\mathbf{k})^2]H + \gamma_b \mathbf{n}_\parallel \mathbf{n}_\parallel : \mathbf{m}. \tag{F5}$$

Equations (F1)–(F5) show that the solid contributions to capillary pressure enters in all four contributions. For finite $\mathbf{b}_s$, this capillary pressure vanishes only if $\mathbf{m}=\mathbf{0}$ and $\mathbf{n}=\mathbf{k}$, or in other words, flat interfaces with homeotropic ($\mathbf{n}=\mathbf{k}$) orientation states. When $\gamma_c=0, \mathbf{b}_s=0$, the results agree with previous work [41].

[1] *Handbook of Liquid Crystal Research*, edited by P. J. Collins and J. S. Patel (Oxford University Press, New York, 1997).
[2] D. Demus, J. Goodby, G. W. Gray, H.-W. Spiess, and V. Vill, *Handbook of Liquid Crystals* (Wiley-VCH, Chichester, NY, 1998).
[3] P. S. Drzaic, *Liquid Crystal Dispersions* (World Scientific, Singapore, 1995).
[4] R. H. Hurt and Z. Y. Chen, Phys. Today **53**, 39 (2000).
[5] J. J. Skaife and N. L. Abbottt, Langmuir **16**, 3529 (2000); J. M. Brake, M. K. Daschner, Y.-Y. Luk, and N. L. Abbott, Science **302**, 2094 (2003).
[6] G. H. Brown and J. J. Wolken, *Liquid Crystals and Biological Structures* (Academic, New York, 1979); A. C. Neville, *Biology of Fibrous Composites* (Cambridge University Press, New York, 1993); P. R. Shewry, A. S. Tatham, and A. J. Bailey, *Elastomeric Proteins* (Cambridge University Press, Cambridge, U.K., 2003).
[7] J. C. Eriksson and S. Ljunggren, Surfactant Sci. Ser. **119**, 547 (2004).
[8] S. H. J. Idziak, I. Koltover, J. N. Israelavhvili, and C. R. Safinya, Phys. Rev. Lett. **76**, 1477 (1996).
[9] P.-G. de Gennes, F. Brochard-Wyart, and D. Quere, *Capillary and Wetting Phenomena* (Springer-Verlag, New York, 2004).
[10] M. E. R. Shanahan, J. Phys. D **21**, 981 (1988).
[11] M. E. R. Shanahan and A. Carre, Colloids and Interfaces A **206**, 115 (2002).
[12] D. J. Srolovitz and S. H. Davis, Acta Mater. **49**, 1005 (2001).
[13] M. A. Fortes, J. Colloid Interface Sci. **100**, 17 (1983).
[14] L. R. White, J. Colloid Interface Sci. **258**, 82 (2003).
[15] A. Sanfeld and A. Steinchen, J. Non-Equilib. Thermodyn. **28**, 115 (2003).
[16] J. M. Howe, *Interfaces in Materials* (Wiley, New York, 1997).
[17] A. Onuki, *Phase Transition Dynamics* (Cambridge University Press, Cambridge, U.K., 2002).
[18] L. B. Feund and S. Suresh, *Thin Film Materials* (Cambridge University Press, Cambridge, UK, 2003).
[19] A. P. Sutton and R. W. Balluffi, *Interfaces in Crystalline Materials* (Oxford, Clarendon Press, New York, 1995).
[20] A. A. Sonin, *The Interface Physics of Liquid Crystals* (Gordon and Breach, Amsterdam, 1995).
[21] H. Yokoyama, in *Handbook of Liquid Crystal Research*, edited by P. J. Collins and J. S. Patel (Oxford University Press, New York, 1997), Chap. 6, p. 179.
[22] P. G. de Gennes and J. Prost, *The Physics of Liquid Crystals*, 2nd ed. (Oxford University Press, London, 1993).
[23] D. A. Edwards, H. Brenner, and D. T. Wasan, *Interfacial Transport Processes and Rheology* (Butterworth-Heinemann, Stoneham, 1991).
[24] J. C. Slattery, *Interfacial Transport Phenomena* (Springer-Verlag, New York, 1990).

[25] J. D. Eliassen, Ph.D. thesis, University of Minnesota, 1963 (University Microfilms, Ann Arbor, 1983).
[26] (a) F. M. Leslie, in *Physical Properties of Liquid Crystals: Nematics*, edited by D. A. Dunmur, A. Fukuda, and G. R. Luckhurst (INSPEC, London, 2001); (b) D. Lhuillier and A. D. Rey, J. Non-Newtonian Fluid Mech. **120**, 169 (2004).
[27] A. D. Rey, Liq. Cryst. **28**, 549 (2001); Phys. Rev. E **67**, 011706 (2003).
[28] T. J. Sluckin and A. Poniewierski, in *Fluid Interfacial Phenomena*, edited by C. A. Croxton (Wiley, Chichester, 1986), Chap. 5.
[29] A. K. Sen and D. E. Sullivan, Phys. Rev. A **35**, 1391 (1987).
[30] M. A. Osipov and S. Hess, J. Chem. Phys. **99**, 4181 (1993).
[31] C. Papenfuss and W. Muschik, Mol. Cryst. Liq. Cryst. Sci. Technol., Sect. A **262**, 561 (1995).
[32] E. G. Virga, *Variational Theories for Liquid Crystals* (Chapman Hall, London, 1994).
[33] J. T. Jenkins and P. J. Barrat, Appl. Math. (Germany) **27**, 111 (1974).
[34] G. Barbero and G. Durand, in *Liquid Crystals in Complex Geometries*, edited by G. P. Crawford and S. Zumer (Taylor and Francis, London, 1996).
[35] B. Jerome, in *Handbook of Liquid Crystals, Vol. 1*, edited by D. Demus, J. Goodby, G. W. Gray, H.-W. Spiess, and V. Vill (Wiley-VCH, Weinheim, 1998).
[36] Q. Wang and G. Forest, Phys. Lett. A **245**, 518 (1998).
[37] J. T. Jenkins, SIAM J. Appl. Math. **32**, 755 (1977).
[38] A. D. Rey, Phys. Rev. E **61**, 1540 (2000).
[39] D. W. Hoffman and J. W. Cahn, Interface Sci. **31**, 368 (1972); J. W. Cahn and D. W. Hoffman, Acta Metall. **22**, 1205 (1974).
[40] A. A. Wheeler and G. B. McFadden, Proc. R. Soc. London, Ser. A **453**, 1611 (1997).
[41] A. G. Cheong and A. D. Rey, J. Chem. Phys. **117**, 5062–5071 (2002).
[42] A. G. Cheong and A. D. Rey, Phys. Rev. E **66**, 021704 (2002).
[43] A. Libai and J. G. Simmonds, *The Nonlinear Theory of Elastic Shells*, 2nd ed. (Cambridge University Press, Cambridge, U.K., 1998).
[44] D. J. Steigmann, in *Nonlinear Elasticity*, edited by Y. B. Fu and R. W. Ogden (Cambridge University Press, Cambridge, U.K., 2001), p. 268.